ORIGINAL RESEARCH

miR-181c Activates Mitochondrial Calcium Uptake by Regulating MICU1 in the Heart

Hemanth N. Banavath, PhD;* Barbara Roman, PhD;* Nathan Mackowski, BS; Debjit Biswas, BS; Junaid Afzal, MBBS; Yohei Nomura, MD; Soroosh Solhjoo, PhD; Brian O'Rourke, PhD; Mark Kohr, PhD; Elizabeth Murphy, PhD; Charles Steenbergen, MD, PhD; Samarjit Das, PhD

***Background*—**Translocation of miR-181c into cardiac mitochondria downregulates the mitochondrial gene, mt-COX1. miR-181c/d$^{-/-}$ hearts experience less oxidative stress during ischemia/reperfusion (I/R) and are protected against I/R injury. Additionally, miR-181c overexpression can increase mitochondrial matrix Ca^{2+} ($[Ca^{2+}]_m$), but the mechanism by which miR-181c regulates $[Ca^{2+}]_m$ is unknown.

***Methods and Results*—**By RNA sequencing and analysis, here we show that hearts from miR-181c/d$^{-/-}$ mice overexpress nuclear-encoded Ca^{2+} regulatory and metabolic pathway genes, suggesting that alterations in miR-181c and mt-COX1 perturb mitochondria-to-nucleus retrograde signaling and $[Ca^{2+}]_m$ regulation. Quantitative polymerase chain reaction validation of transcription factors that are known to initiate retrograde signaling revealed significantly higher Sp1 (specificity protein) expression in the miR-181c/d$^{-/-}$ hearts. Furthermore, an association of Sp1 with the promoter region of MICU1 was confirmed by chromatin immunoprecipitation-quantitative polymerase chain reaction and higher expression of MICU1 was found in the miR-181c/d$^{-/-}$ hearts. Conversely, downregulation of Sp1 by small interfering RNA decreased MICU1 expression in neonatal mouse ventricular myocytes. Changes in PDH activity provided evidence for a change in $[Ca^{2+}]_m$ via the miR-181c/MICU1 axis. Moreover, this mechanism was implicated in the pathology of I/R injury. When MICU1 was knocked down in the miR-181c/d$^{-/-}$ heart by lentiviral expression of a short-hairpin RNA against MICU1, cardioprotective effects against I/R injury were abrogated. Furthermore, using an in vitro I/R model in miR-181c/d$^{-/-}$ neonatal mouse ventricular myocytes, we confirmed the contribution of both Sp1 and MICU1 in ischemic injury.

***Conclusions*—**miR-181c regulates mt-COX1, which in turn regulates MICU1 expression through the Sp1-mediated mitochondria-to-nucleus retrograde pathway. Loss of miR-181c can protect the heart from I/R injury by modulating $[Ca^{2+}]_m$ through the upregulation of MICU1. **(*J Am Heart Assoc*. 2019;8:e012919. DOI: 10.1161/JAHA.119.012919.)**

Key Words: microRNA • miRNA • mitochondria • mitomiR • mitochondrial calcium • heart failure

Mitochondrial Ca^{2+} transport is an important mechanism to maintain cellular Ca^{2+} homeostasis, which further determines mitochondrial bioenergetic capacity and cellular fate. Increased mitochondrial matrix Ca^{2+} ($[Ca^{2+}]_m$) has been shown to be an important regulator of mitochondrial function by simultaneously activating both Krebs cycle enzymes and oxidative phosphorylation[1] to increase ATP production, but it also plays a role in various disease processes. Increasing $[Ca^{2+}]_m$ can increase mitochondrial reactive oxygen species (ROS) scavenging during increases in workload, but excessive Ca^{2+} loads can trigger opening of the permeability transition pore.[2,3] The mitochondrial calcium uniporter (MCU) forms a complex with several regulatory proteins (MCUR1, EMRE, MICU1 and MICU2), and the

From the Departments of Pathology (H.N.B., B.R., D.B., S.S., C.S., S.D.) and Anesthesiology & Critical Care Medicine (S.D.), Division of Cardiac Surgery, Department of Surgery (Y.N.), and Division of Cardiology, Department of Medicine (S.S., B.O.), Johns Hopkins School of Medicine, Baltimore, MD; Department of Environmental Health and Engineering, Johns Hopkins Bloomberg School of Public Health, Baltimore, MD (N.M.); Department of Medicine, UCSF School of Medicine, San Francisco, CA (J.A.); Cardiac Physiology Section, National Heart, Lung, and Blood Institute, NIH, Bethesda, MD (E.M.).

Accompanying Figures S1 through S4 are available at https://www.ahajournals.org/doi/suppl/10.1161/JAHA.119.012919

*Dr Banavath and Dr Roman contributed equally to this work.

Correspondence to: Samarjit Das, PhD, and Charles Steenbergen, MD, PhD, Department of Anesthesiology & Critical Care Medicine, Cardiovascular Division, Department of Pathology, Johns Hopkins School of Medicine, Baltimore, MD 21205. E-mails: sdas11@jhmi.edu; csteenb1@jhmi.edu

Received August 20, 2019; accepted November 5, 2019.

Clinical Perspective

What Is New?

- Novel bidirectional nuclear-mitochondrial communication pathway, involving a microRNA.
- Novel mechanism by which MICU1 expression can be regulated in the heart.

What Are the Clinical Implications?

- MicroRNAs can be involved in nuclear-mitochondrial communication, which may be an adaptive response but could become maladaptive in a variety of forms of heart disease including susceptibility to myocardial ischemia-reperfusion injury.

mitochondrial membrane potential ($\Delta\Psi_m$) drives $[Ca^{2+}]_m$ entry through the MCU channel.[4–9] MCU and its regulatory proteins form a complex network to control Ca^{2+} entry into the mitochondria. There are several studies establishing the importance of MCU and its regulatory proteins in $[Ca^{2+}]_m$.[5,7,9–12] However, the detailed mechanisms by which expression of MCU or its regulatory proteins are regulated in the heart under physiological conditions are not fully understood.

Alterations in the ratio of MICU1 to MCU lead to changes in calcium uptake threshold and cooperativity.[11] MICU1 was the first regulatory MCU complex member identified and shown to play an important role in $[Ca^{2+}]_m$ responses.[13] Three isoforms of MICU (MICU1, MICU2, and MICU3) localize in the intermembrane space and control the opening of MCU.[14,15] MICU1 changes MCU to the closed conformation at low cytoplasmic Ca^{2+} ($[Ca^{2+}]_{cyto}$)[9,14,15] and also contributes to the open conformation at high $[Ca^{2+}]_{cyto.}$[15] Data from cell culture models where MICU1 has either been knocked down or knocked out have offered somewhat conflicting results. For example, knockdown of MICU1 does not alter $[Ca^{2+}]_m$ after treatment with a compound which increases $[Ca^{2+}]_{cyto.}$[9] On the other hand, it has been shown that MICU1 knockout cells have dysregulated $[Ca^{2+}]_m$ uptake at low $[Ca^{2+}]_{cyto}$.[13,14] Several research groups have reported that genetic deletion of MICU1 can lead to baseline $[Ca^{2+}]_m$ overload.[9,16] However, others have not observed this.[13,14,17] Most agree MICU1 inhibits mitochondrial Ca^{2+} entry at low $[Ca^{2+}]_{cyto}$, and activates mitochondrial Ca^{2+} entry at high $[Ca^{2+}]_{cyto}$.[10,18] Although there are controversies concerning how MICU1 regulates mitochondrial calcium uptake, it is clear that MICU1 can affect $[Ca^{2+}]_m$, and this could be even more important under pathophysiological stress conditions. Several studies have focused on the roles of MCU and MCU regulatory proteins, such as MICU1, in cardiovascular pathophysiology.[4–9] However, the mechanisms that regulate MICU1 expression are unknown. It is also not known how MICU1 is regulated under pathophysiological conditions. In this study, we will test the hypothesis that changes in complex IV (mt-COX1), attributable to alterations in miR-181c expression, impact the rate of ROS production, which alters a transcription factor, Sp1 (specificity protein 1), in turn modulating MICU1 expression.

miR-181c is encoded in the nuclear genome and translocates to the mitochondria. Importantly, it regulates mitochondrial gene expression by directly binding to the 3′ end of mt-COX1.[19–21] miR-181c mainly localizes to the mitochondrial compartment of cardiomyocytes,[20,22,23] regulates mitochondrial function in the heart, and influences myocardial injury by increasing mitochondrial production of ROS.[19,20,22] Nuclear factor erythroid 2–related factor 2/NRF2 activity has been demonstrated to stimulate miR-181c transcription.[21] NRF2 regulates the expression of antioxidant proteins that protect against oxidative damage triggered by multiple metabolic stressors.[24] Several metabolic conditions, such as aging, obesity, type 2 diabetes mellitus, and neurodegenerative disease, are characterized by higher expression of miR-181c in the mitochondrial compartment. In this study, we demonstrate that by regulating mt-COX1, miR-181c alters ROS, which alters Sp1 expression, which ultimately regulates MICU1 expression.

Methods

Per the Transparency and Openness Promotion (TOP) Guidelines, the data, analytic methods, and study materials will be available to other researchers on request to the corresponding author.

Animals

miR-181c/$d^{-/-}$ mice were generated on the BL6 background.[22] Male C57BL6/J (Jackson Laboratories, Bar Harbor, ME) were used as wild-type (WT) control for miR-181c/$d^{-/-}$ mice. We used 12-week-old male mice for all of our studies. They were provided with food and water ad libitum. Mice were treated humanely, and all experimental procedures were approved by the Institutional Animal Care and Use Committee of the Johns Hopkins University.

Neonatal Mouse Ventricular Myocyte Isolation and Culture

Heart tissue from both WT (C57BL6/J) and miR-181c/$d^{-/-}$ knock-out mice pups postnatal day 0 to day 3 (P_0–P_3) was dissociated using Neonatal Heart Dissociation Kit (Miltenyi Biotec, Auburn, CA). Neonatal mouse ventricular myocytes (NMVMs) were isolated from the heart cell homogenate by

magnetic labeling of noncardiomyocytes using Neonatal Cardiomyocyte Isolation Kit (Miltenyi Biotec, Auburn, CA), following the company's instruction. Isolated NMVMs were cultured on fibronectin-coated cover glasses and supplemented with Medium 199 containing 2% fetal bovine serum and 100 U of penicillin G/mL and kept in a humidified incubator at 37°C in 5% CO_2.

H9c2 Cell Culture

H9c2 myoblastic cells were maintained in Dulbecco's Modified Eagle's medium supplemented with 10% fetal bovine serum, 100 U of penicillin G/mL, and 100 μg of streptomycin/mL and maintained at 37°C in 5% CO_2.

Chromatin Immunoprecipitation Assay

Either mouse heart tissue or H9c2 cells were incubated in 1% formaldehyde for 10 minutes and then swirled and incubated in 10X glycine solution for 5 minutes. Cells or tissue were washed twice in PBS and resuspended in 1X Buffer A, 1M DTT, and 200x PIC from SimpleChIP Plus Enzymatic Chromatin IP Kit (Cell Signaling Technology, Danvers, MA). Sample homogenates were then incubated in micrococcal nuclease for 20 minutes in 37°C with frequent mixing. Digestion was terminated by adding 0.5 mol/L EDTA and moving the samples to ice. Chromatin was sonicated in 3 sets of 10-second pulses using a probe sonicator. Excess debris was removed by centrifugation in 4°C for 10 minutes. Samples were then incubated for 30 minutes at 37°C in nuclease-free water, 5 mol/L NaCl, and RNAse A. Proteinase K was then added to each RNAase A–digested sample and incubated at 65°C for 2 hours. DNA was purified and digested to 150 to 900 bp. 1X chromatin immunoprecipitation (ChIP) buffer and 200X PIC was added to each chromatin sample, followed by a 2 hours incubation in ChIP-Grade Protein G Agarose Beads at 4°C with rotation. Chromatin was washed 3 times with low-salt wash and 1 time with high-salt wash. Samples were centrifuged, and the supernatants were removed. Samples were eluted from the Protein G Agarose Beads conjugated with Sp1 antibody (Sigma-Aldrich, Cat# AV37192) by mixing them in 1X ChIP elution buffer for 30 minutes at 65°C. Crosslinks were reversed by incubating samples for 2 hours at 65°C in 5 mol/L NaCl and proteinase K. DNA was purified and quantified by polymerase chain reaction (PCR).

RNA Isolation

Total RNA was isolated from whole hearts or NMVMs or from H9c2 cell line using a miRNeasy kit (Qiagen, Valencia, CA) and RNase free DNase kit (Qiagen, Valencia, CA).[20] To characterize the integrity of the isolated RNA, spectrophotometric evaluation was performed, using Nanodrop (Thermo Scientific, Wilmington, DE). Only RNA samples whose A_{260} (absorbance at 260 nm) value was >0.15 were used for further experiments. The ratio of the readings A_{260}/A_{280} was also evaluated in order to check the purity of the isolated RNA.

Quantitative Real-Time PCR

After performing the purity and integrity test, the RNA was reverse transcribed using a miScript Reverse Transcription Kit (Qiagen, Valencia, CA). Polymerase chain reaction (PCR) was performed using a miScript SYBR green PCR kit (Qiagen, Valencia, CA) and detected with a CFX96 detector (Bio-Rad, Hercules, CA). All reactions were performed in triplicate. Table shows all the primer sequences for the mitochondria encoded genes.

Transfection

miR-181c overexpression was performed by transient transfection using either scramble (Scr, Qiagen) or miR-181c mimic (Cat# MIMAT0000674, Qiagen) in H9c2 or NMVMs. In vitro knocking down of Sp1 or MICU1 expression was performed using small interference RNAs against Sp1 (siSp1; ON-TARGET*plus* SMART Pool Cat# L-040633-02-0005, Dharmacon, Lafayette, CO) and MICU1 (siMICU1; ON-TARGET*plus* SMART Pool Cat# L-053388-01, Dharmacon, Lafayette, CO). Both siSp1 and siMICU1 transfected groups were compared with scramble (siScr, ON-TARGET*plus* Non-targeting Control siRNA #1, Cat# D-001810-01-05, Dharmacon, Lafayette, CO) transfected group. All transfections were carried out using Lipofectamine RNAiMAX (Thermo Fisher Scientific, Waltham, MA).

Pyruvate Dehydrogenase Activity

The catalytic activity of pyruvate dehydrogenase (PDH) in NMVMs, H9c2 cells, or heart tissue was determined by PDH Enzyme Activity Microplate Assay Kit (Cat# ab109902, Abcam, Cambridge, MA) following the manufacturer's instruction.

Generation of MICU1-Lentivirus Complex for In Vivo Delivery

MICU1 targeting (Cat#: TL512307) and scrambled control (Cat#: TR30021) short-hairpin RNA plasmids were obtained from OriGene Technologies, Inc (Rockville, MD). Lentiviruses were generated using Lenti-vPack Lentiviral Packaging Kit (OriGene Technologies, Rockville, MD) following the manufacturer's instructions. Briefly, 2×10^6 HEK293FT cells were transfected with 6 μg of packaging plasmids mix and 5 μg of shMICU1 plasmid or 5 μg of control shScramble plasmid

Table. Primer Sequences for qPCR

Target	Forward	Reverse
ATF2	ACATCCAATGGAGTCAGTTC	GCCATGACAATCTGTGAAAG
EGR1	TTGTGGCCTGAACCCCTTTT	AGATGGGACTGCTGTCGTTG
HIF1α	TCAAGTCAGCAACGTGGAAG	TATCGAGGCTGTGTCGACTG
mTOR	GCAGAAGGTAGAGGTGTTTGAGCAT	GTATCCGACCATCGACATAACGG
MYC	GGGCTTTATCTAACTCGCTGTA	GCTATGGGCAAAGTTTCGTG
NFATC1	CATGCGCCCTCTGTGGCCC	GGAGCCTTCTCCACGAAAATG
NRF2	TCTTGGAGTAAGTCGAGAAGTGT	GTTGAAACTGAGCGAAAAAGGC
PGC1α	AAGGTCCCCAGGCAGTAGAT	GCGGTATTCATCCCTCTTGA
STAT3	ACCCAACAGCCGCCGTAG	CAGACTGGTTGTTTCCATTCAGAT
SIRT3	AGGTGGAGGAAGCAGTGAGA	CGGGATGTCATACTGCTGAA
Sp1	CATGCCAGGCCTCCAGAC	CACCAGATCCATCAAGACCAAGTT
MICU1	AACAGCAAGAAGCCTGACAC	CTCATTGGGCGTTATGGAG
β-Actin	GGGCTGTATTCCCCTCCATCG	CCAGTTGGTAACAATGCCATG

qPCR indicates quantitative polymerase chain reaction.

using Lipofectamine 3000 (Thermo Fisher Scientific). Cell culture media was changed after 12 hours of transfection and supernatant was collected at 48 and 72 hours following transfection. Supernatant media was filtered through 0.45 μmol/L filter, 33 mm diameter polyvinylidene fluoride syringe filter (Centricon Plus-70 filter units, Millipore, USA) and purified using Fast-Trap Lentivirus Purification and Concentration Kit (Millipore, USA). The final elution of viruses was done in PBS and various aliquots were frozen. The viral titer was determined using Lenti-X p24 Rapid Titer Kit (Takara Bio USA, Mountain View, CA) after thawing 1 of the aliquots from the PBS stock. We have validated almost 40% knock-down of MICU1 in the NMVM when NMVM was incubated with shMICU1 for 48 hours (Figure S1).

Cardiac-lentivirus delivery protocol was optimized through the jugular vein delivery. Packaged short-hairpin RNA, either shScramble or against MICU1 (shMICU1) into a lentivirus were injected at a dose of 10^6 viral particles/injection (3 times over 1 week) into miR-181c/d$^{-/-}$ and WT mice. We used 50 μL PBS to dilute 10^6 viral particles. The injections were performed every alternate day in alternate veins. Two weeks after the first injection, the mice were euthanized, and cardiac-MICU1 expression was determined.

Langendorff Mouse Heart Preparation

After sufficient anesthesia was achieved with ketamine (90 mg/kg body weight)/xylazine (10 mg/kg body weight) intraperitoneal cocktail, and the mouse was anticoagulated with heparin sodium (500 IU/kg body weight, intravenous injection) (Elkin-Sinn Inc, Cherry Hill, NJ), mouse hearts were excised, cannulated, and perfused with Krebs-Henseleit buffer containing (in mmol/L) NaCl 120, KCl 5.9, $MgSO_4$ 1.2, $CaCl_2$ 1.25, $NaHCO_3$ 25, and glucose 11. The buffer was aerated with 95% O_2 and 5% CO_2, to give a pH of 7.4 at 37°C as described previously.[25] All hearts were perfused to wash out blood and stabilized for 20 minutes, followed by 20 minutes of global ischemia and 120 minutes of reperfusion. Left ventricular developed pressure and heart rate were continuously monitored via a water-filled balloon inserted into the left ventricle. Recovery of contractile function was assessed by measurement of left ventricular developed pressure during reperfusion and was expressed as a percentage of preischemic, pretreatment left ventricular developed pressure.

At the end of reperfusion, infarct size was measured with 2,3,5-triphenyltetrazolium chloride as described previously.[25] Hearts were initially perfused with 2,3,5-triphenyltetrazolium chloride and then incubated in 2,3,5-triphenyltetrazolium chloride solution for an additional 15 minutes at 37°C. The hearts were subsequently fixed in formalin, followed by 4 to 6 cross-sectional slices were cut. These slices were imaged on a Leica Stereoscope, and the percentage of infarct (white area) to viable tissue (red area) was analyzed using ImageJ software. Area of infarct was expressed as a percentage of the total ventricles.

Whole Hearts or NMVM Preparation for Western Blot

Whole heart, NMVM, or H9c2 cell lysate samples were lysed with radioimmunoprecipitation assay buffer and protein

contents were measured using a Bradford assay.[19] Protein samples and molecular weight standards were separated by 1D gel electrophoresis. After transfer to a polyvinylidene fluoride membrane, the membranes were incubated with antibody that recognizes proteins such as mt-COX-1 (Cat# ab203912), MCU (Cat# ab121499), PDH (Cat# ab110330), and α-Tubulin (Cat# ab7291) from Abcam (Cambridge, MA), Sp1 (Cat# AV37192) from Sigma-Aldrich (St. Louis, MO); and MCUR1 (Cat# 13706S), PGC-1α (Cat# 2178S), MICU1 (Cat# 12524S) from Cell Signaling Technologies (Danvers, MA), and EMRE (Cat# sc86337) from Santa Cruz Biotechnology (Dallas, TX), in Tris-Buffered Saline (pH 7.4) with 1% TWEEN 20 (TBS-T) with 5% BSA or nonfat dry milk at 4°C overnight. Membranes were incubated with the secondary antibody, appropriate horseradish peroxidase–conjugated IgG in TBS-T with 5% nonfat dry milk for 1 hour at room temperature. Immunoreactive protein was visualized using an enhanced chemiluminescence analysis kit (GE HealthCare, Piscataway, NJ).

RNA Sequencing and Data Analysis

The quality of the paired-end reads was assessed using FastQC tools.[26] Adapter sequences and low-quality bases were trimmed using Cutadapt.[27] Reads were mapped to mouse genome using STAR version 2.6.1c,[28] which aligns reads to the known transcriptome and genome using the splice-aware aligner. Only uniquely mapped paired-end reads were then used for subsequent analyses. FeatureCounts[29] was used for gene-level abundance estimation using the GENCODE[30] vM11 comprehensive gene annotations. Principal component analysis was used to assess outlier samples. The read counts were filtered if they had <5 counts across half the samples. Differential expression analysis comparing cases versus controls at the gene levels of summarization were then carried out using open source Limma R package.[31] Limma-voom[32] was employed to implement a genewise linear modeling, which processes the read counts into log2 counts per million with associated precision weights. The log2 counts per million values were normalized between samples using trimmed mean of M values.[33] We adjust for multiple testing by reporting the false discovery rate q values for each feature.[34] Features with q <5% were declared as genome-wide significant. We then used the R statistical software environment using the GAGE Bioconductor packages[35] to carry out the analyses on predefined gene ontology gene sets by conducting two sample t tests on the log-based fold changes of target gene set and control sets. The gene ontology categories included were biological process, cellular component and molecular function. False discovery rate q values were estimated to correct the *P* values for the multiple testing issue.

Statistical Analysis

The results are presented as mean and standard error of the mean (mean±SEM). For sample size 6 (n=6) we used the Student *t* test to calculate *P* value. $P<0.05$ was considered statistically significant. For multiple comparisons, 2-way ANOVA and the Bonferroni post hoc test were used. $P<0.05$ was considered statistically significant. All analyses were performed using Prism 5 (GraphPad Software Inc, CA).

Results

miR-181c Regulates Mitochondria-to-Nuclear Retrograde Signaling

miR-181c overexpression led to downregulation of mitochondrial complex IV, and activated mitochondrial O_2 consumption, which involved increased $[Ca^{2+}]_m$.[19] To explore the mechanism by which miR-181c targets mt-COX1 and increases $[Ca^{2+}]_m$, we performed RNA sequencing using total RNA from the hearts of WT (C57BL6) and miR-181c/$d^{-/-}$ mice. Principal component analysis clearly distinguishes the 2 groups (Figure 1A). Further bioinformatics analysis suggests that the cellular Ca^{2+} activated (both cytosolic and mitochondrial) pathway is significantly upregulated in the miR-181c/$d^{-/-}$ group (Figure 1B). Almost all of the mRNAs in this pathway analysis are nuclear encoded. This finding suggests that a change in one mitochondrial protein can activate mitochondria-to-nucleus retrograde signaling in cardiomyocytes. To further examine this, we interrogated known transcription factors, which are involved in mitochondria-to-nucleus retrograde signaling, using quantitative PCR (Figure 1C). Sp1 and PGC-1α are the top 2 upregulated mRNAs in the miR-181c/$d^{-/-}$ hearts (Figure 1C). Western blot analysis also validated the upregulation of Sp1 protein in miR-181c/$d^{-/-}$ (Figure 1D). Several studies have implicated a potential role for mitochondrial ROS in the repression of Sp1 expression.[36–38] Taken together, our data suggest that overexpressing mt-COX1 through lowered miR-181c reduces mitochondrial ROS production, which then stimulates mitochondria-to-nuclear retrograde signaling possibly through activation of Sp1.

miR-181c Alters MICU1 Transcription Through Sp1 Expression

In the human heart, it has been shown that activating Sp1 can directly upregulate MICU1 transcription by binding to the promoter region of MICU1.[39] Therefore, we hypothesize that lowering miR-181c expression in hearts from miR-181c/$d^{-/-}$ mice can increase MICU1 expression through an increase in

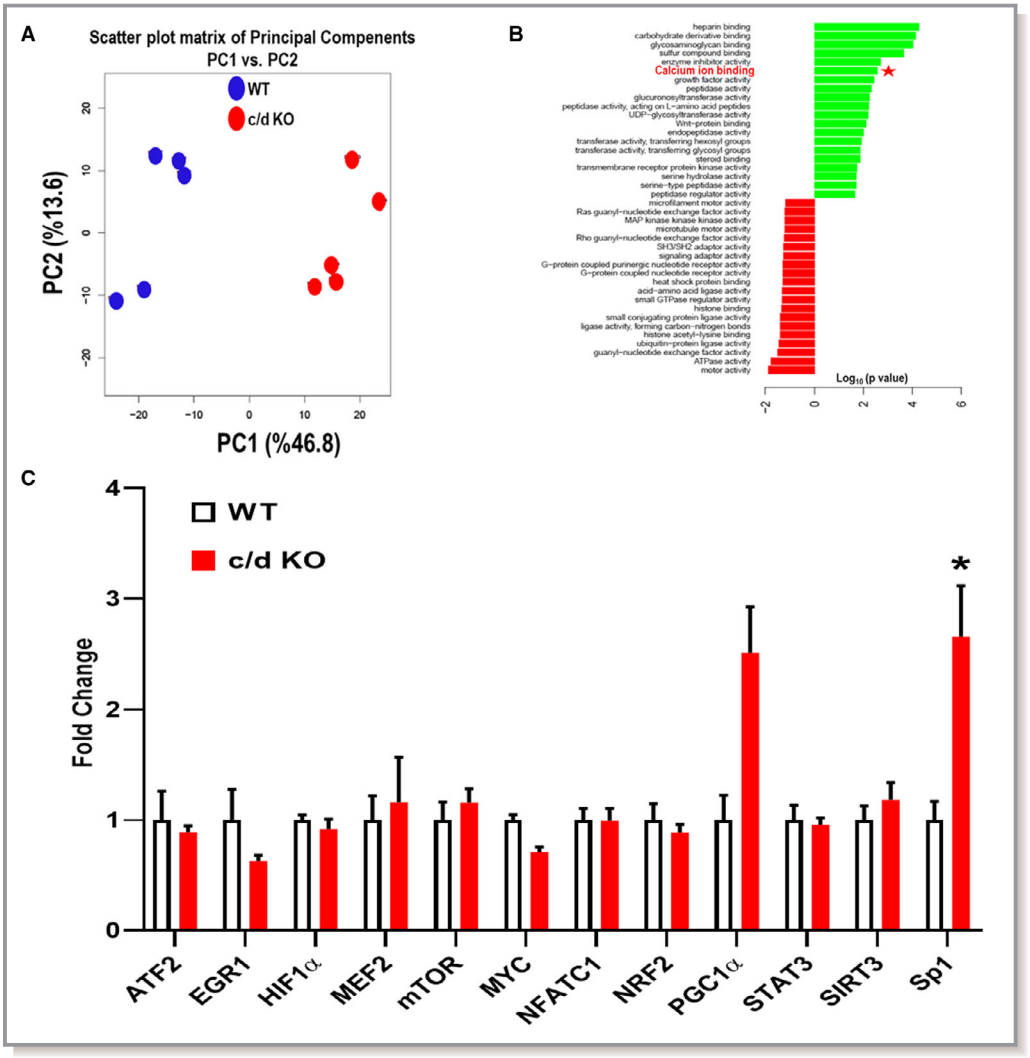

Figure 1. Transcription factor Sp1 mediates miR-181c induced mitochondria-to-nucleus retrograde signal. **A**, Principal component analysis (PCA) was performed on the normalized reads per million data from the RNA sequencing reading. Red dots denote the miR-181c/d$^{-/-}$ groups, and black dots denote WT (C57BL6/j) groups. **B**, The pathway analysis was performed by stimulating the genes, which are either upregulated or downregulated significantly in miR-181c/d$^{-/-}$ hearts compared with WT hearts. **C**, Quantitative PCR (SYBR) validation of all transcription factors, which has potential role in mitochondria-to-nucleus retrograde signaling, from the RNA sequencing data. To correct for multiple comparisons, statistical significance was determined using the Holm-Sidak method, with α=0.05. Each row was analyzed individually, without assuming a consistent SD. Number of t tests: 12. **D**, Western blot analysis of Sp1 expression in heart tissue from WT (C57BL6/j) and miR-181c/d$^{-/-}$ mice. Sp1 (upper bands) expression was normalized to α-Tubulin (lower bands). Chromatin immunoprecipitation (ChIP) was performed from the nuclear fraction of heart tissues from WT and miR-181c/d$^{-/-}$ hearts using Sp1 antibody. **E**, Real-time PCR was performed from the Sp1-associated DNA fractions from both WT and miR-181c/d$^{-/-}$ groups. **F**, Quantitative PCR (SYBR) was performed from the Sp1-associated DNA fractions from both WT and miR-181c/d$^{-/-}$ groups. *P<0.05, vs WT. n=3 to 6. KO indicates knockout; PCR, polymerase chain reaction; Sp1, specificity protein; WT, wild-type.

Sp1 expression (miR-181c↓→mt-COX1↑→ROS↓→Sp1↑→MICU1↑). To test our hypothesis, in-silico analysis was performed and a potential Sp1 binding site was identified, from 996 nt to 1004 nt, in the GC-box region of the mouse MICU1 promoter (Figure S2). ChIP assay was then performed by immunoprecipitation using a Sp1 antibody. After pulldown of the Sp1-bound DNA, both real-time PCR (Figure 1E), and quantitative PCR (Figure 1F) were performed for the GC-box region of the MICU1 promoter. A significantly higher association of Sp1 with the MICU1 promoter region was detected. These data are consistent with the hypothesis that the miR-181c/d$^{-/-}$ heart has higher expression of MICU1, as there

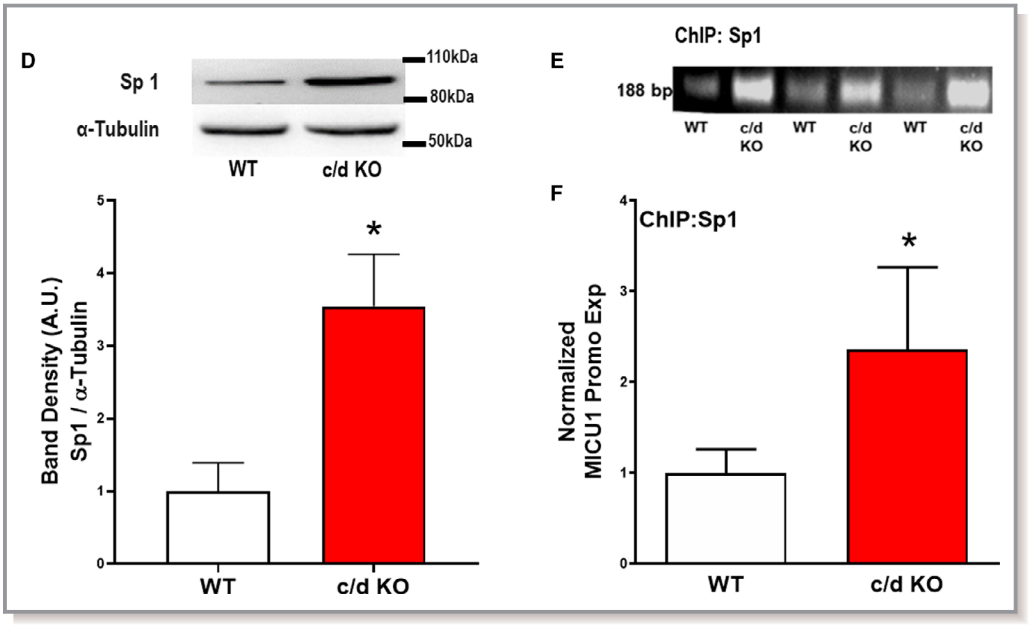

Figure 1. Continued

are significantly higher levels of Sp1/MICU1 promoter region association. To demonstrate this, a western blot for MCU and its regulatory proteins was performed. Indeed, the miR-181c/d$^{-/-}$ mouse heart showed significantly higher MICU1 expression both in mRNA (Figure 2A) and in protein level (Figure 2B), without any alteration in MCU (Figure 2C and 2D) or other MCU regulatory proteins, such as MCUR1 (Figure 2C and 2E) or EMRE (Figure 2C and 2F).

miR-181c Modulates $[Ca^{2+}]_m$ Uptake Attributable to the mt-COX1→Sp1→MICU1 Signaling Pathway

To further validate the signaling pathway by which miR-181c can modulate MICU1 expression in a miR-181c-gain-of-function model, the rat myoblast cell line (H9c2) was used. Mature miR-181c was overexpressed following our previously published protocol, which causes significant activation of ROS production.[20] As expected, mt-COX1 expression was significantly lower in the miR-181c overexpression group compared with the scramble transfected group, 48 hours after transfection (Figure 3A). miR-181c overexpression also downregulated Sp1 expression (Figure 3A), without changing PGC-1α expression (Figure 3A). Bioinformatics analysis (using targetscan and microrna.org) showed that miR-181c could not directly bind to the 3′-UTR of Sp1 mRNA. Therefore, we hypothesize that alteration of Sp1 by miR-181c is through the mt-COX1→ROS pathway. ChIP-quantitative PCR using immunoprecipitation with a Sp1 antibody, showed a significant decrease in Sp1 and MICU1 promoter region association compared with the scramble transfected group (Figure 3B). Indeed, we have identified a significant down-regulation of MICU1 expression with miR-181c overexpression (Figure 3C). To assess whether $[Ca^{2+}]_m$ is altered, we examined direct targets of Ca^{2+} in the mitochondrial matrix such as PDH, which is regulated by a calcium-sensitive dephosphorylation mechanism.[1,40–43] PDH activity is increased in the presence of $[Ca^{2+}]_m$ and the PDH activity was significantly higher in the miR-181c overexpression group 48 hours after transfection (Figure 3D). There was no change of total PDH expression between the 2 groups—Scramble and miR-181c OE (Figure 3E). These data further suggest that miR-181c overexpression can cause MICU1 downregulation through the downregulation of Sp1. We also looked at Sp1 expression with/without antioxidant treatment (Mito-TEMPO 25 nmol/L for 48 hours) in normal (without any stress) H9c2 cells. As shown in Figure S3, Mito-TEMPO does not change Sp1 expression at baseline, suggesting that ROS production is so low at baseline that Mito-TEMPO has no effect. According to our hypothesis, if we activate Sp1 with a small molecule while overexpressing miR-181c, we should nullify the effect of miR-181c on $[Ca^{2+}]_m$ level by directly stimulating the Sp1→MICU1 signaling pathway.

Epicatechin has been shown to activate Sp1 in cardiomyocytes.[44] Overexpression of miR-181c was performed with/without epicatechin (1 μmol/L) in the H9c2 culture media. Consistent with our previous results (Figure 2), miR-181c overexpression significantly downregulates both Sp1 and MICU1 expression (Figure 4A through 4C). However, epicatechin can rescue Sp1 and MICU1 expression following miR-181c overexpression at 48 hours (Figure 4A through 4C). Importantly, significantly lower PDH activity (measure of

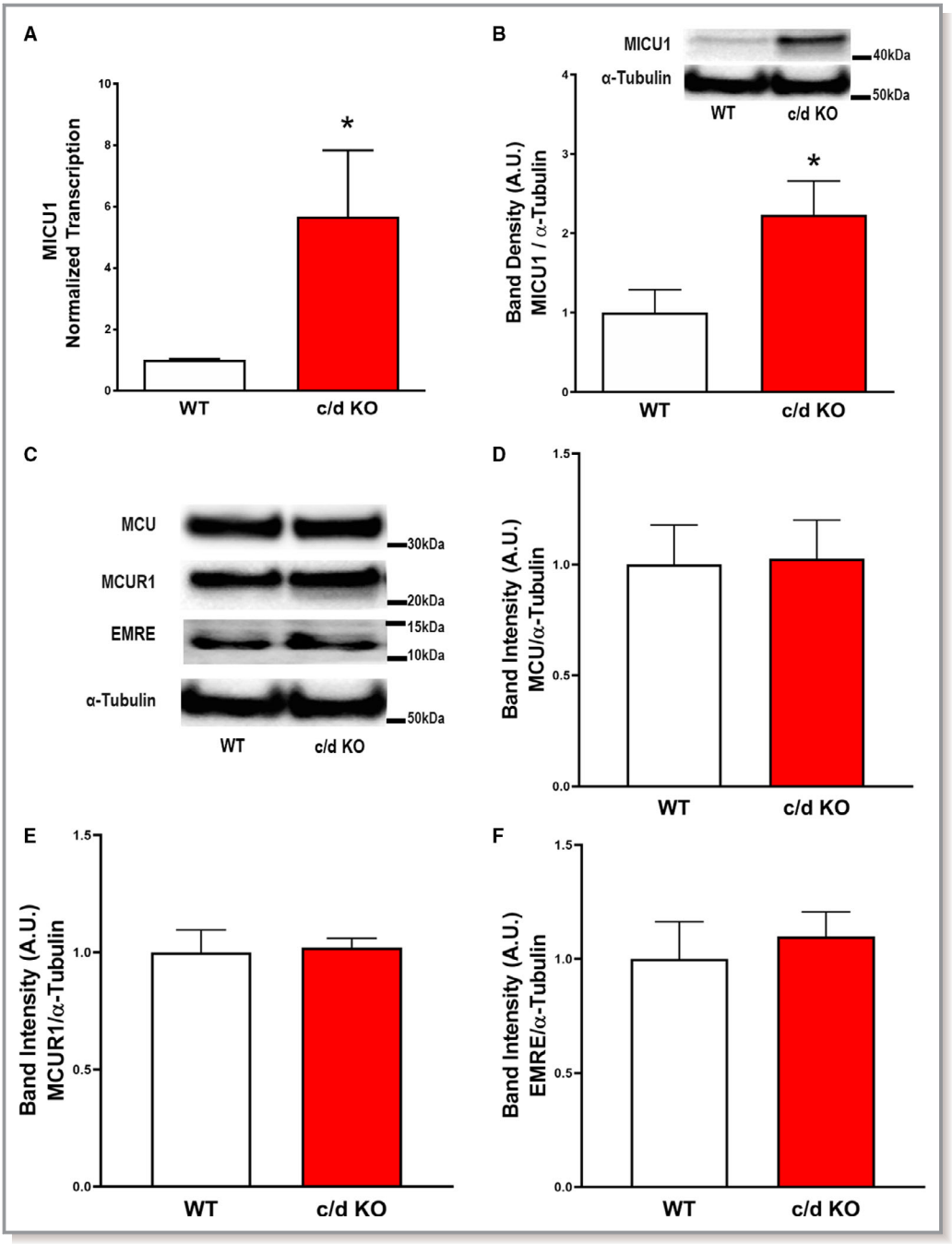

Figure 2. Upregulation of MICU1 in miR-181c/$d^{-/-}$ hearts. **A**, Quantitative PCR (SYBR) was performed from the RNA fractions of WT and miR-181c/$d^{-/-}$ hearts. Western blot analysis of MICU1 expression in heart tissue from WT (C57BL6/j) and miR-181c/$d^{-/-}$ mice. **B**, MICU1 (upper bands) expression was normalized to α-Tubulin (lower bands). Western blot analysis of mitochondrial calcium uniporter (MCU) and other MCU-regulatory proteins, such as MCUR1 (MCU-regulatory protein 1), essential mCU regulator (EMRE) were also performed. **C**, MCU (upper bands), MCUR1 (second bands), and EMRE (third bands) expressions were normalized to α-tubulin (lower bands). **D** through **F**, Bar graphs show the quantification of protein expression. *P<0.05, vs WT. n=6. KO indicates knockout; PCR, polymerase chain reaction; Sp1, specificity protein; WT, wild-type.

$[Ca^{2+}]_m$) was observed in the miR-181c overexpression group treated with epicatechin, compared with the miR-181c overexpression without epicatechin treatment (Figure 4D). These data further support the role of the signaling pathway involving miR-181c↑→mt-COX1↓→ROS↑→Sp1↓→MICU1↓, which then alters $[Ca^{2+}]_m$.

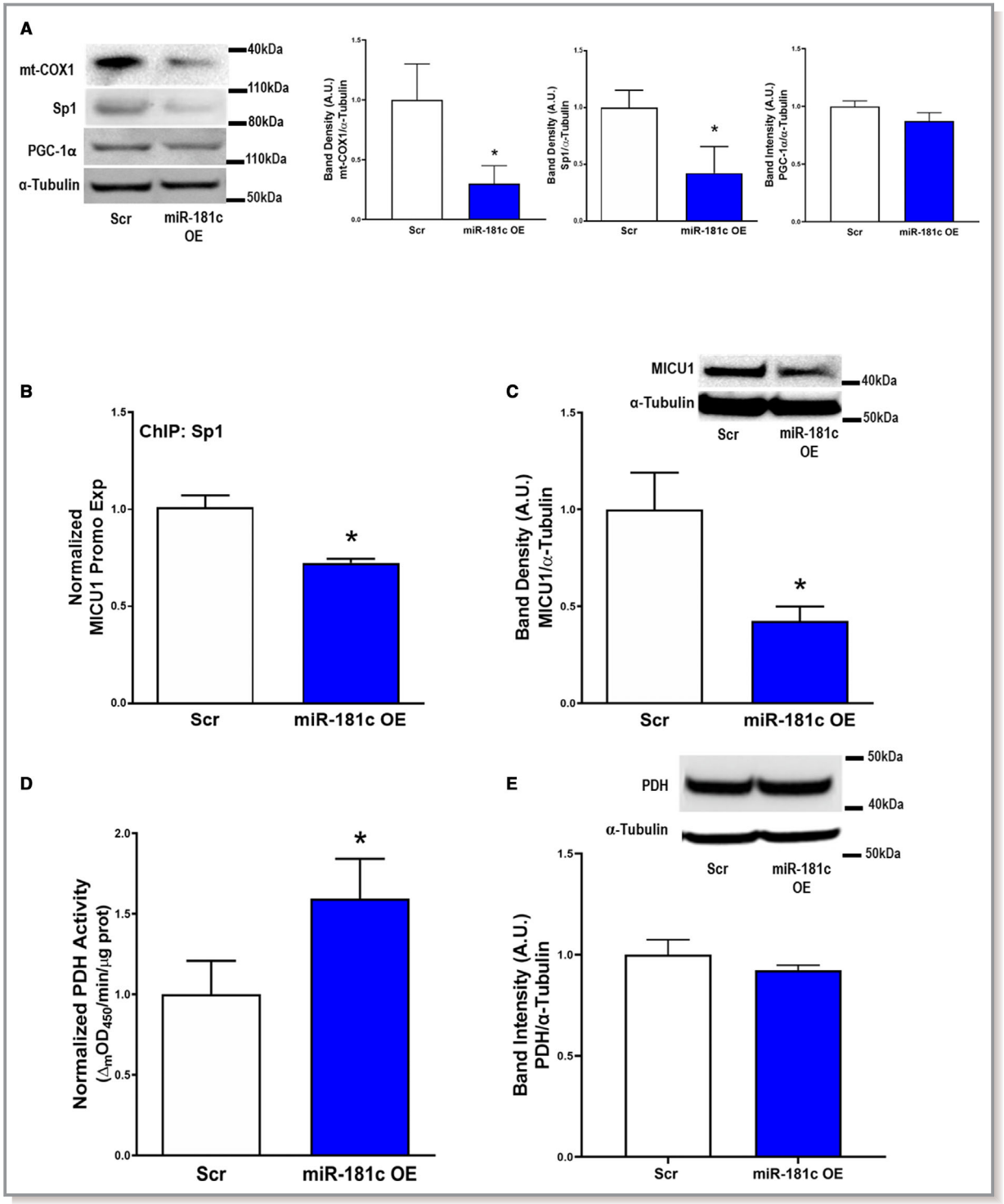

Figure 3. miR-181c overexpression (OE) causes $[Ca^{2+}]_m$ accumulation though MICU1 downregulation. **A**, Western blot analysis of mt-COX1, PGC-1α, and Sp1 expressions in the H9c2 lysates from either Scramble (Scr) or miR-181c mimic (miR-181c OE) transfected groups. mt-COX1 (upper bands), PGC-1α (second bands) and Sp1 (third bands) expression was normalized to α-tubulin (lower bands). **B**, ChIP-qPCR was performed using Sp1 antibody from the H9c2 lysates from either Scr or miR-181c mimic (miR-181c OE) transfected groups. **C**, Western blot analysis of MICU1 expression in the H9c2 lysates from Scr miR-181c mimic (miR-181c OE) transfected groups. MICU1 (upper bands) expression was normalized to α-tubulin (lower bands). **D**, Pyruvate dehydrogenase (PDH) enzyme activity, and **E**, PDH expression, was measured in the H9c2 lysates from Scr miR-181c mimic (miR-181c OE) transfected groups. *P<0.05, vs WT. n=3 to 6. ChIP-qPCR indicates chromatin immunoprecipitation–quantitative polymerase chain reaction; PGC-1α, peroxisome proliferator–activated receptor g coactivator-1 α; Sp1, specificity protein.

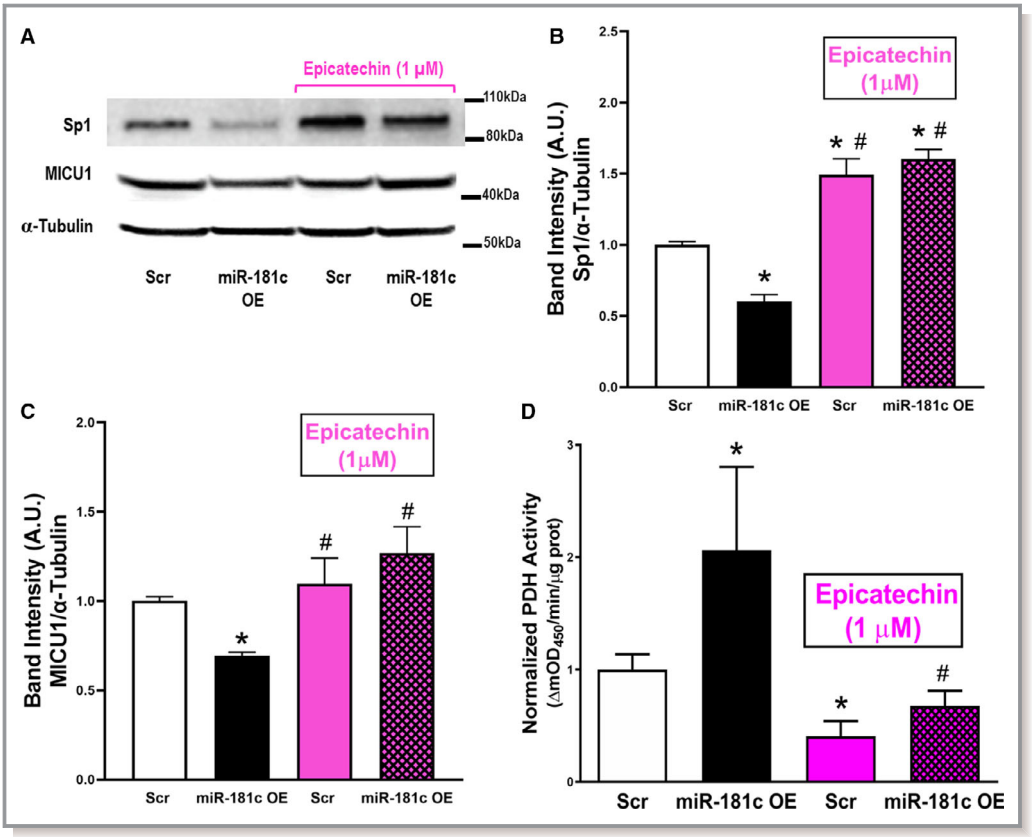

Figure 4. miR-181c effect on MICU1 expression can be altered by activating Sp1. The scramble (Scr) or miR-181c mimic (miR-181c OE) transfected H9c2-cells were treated with/without epicatechin (1 μmol/L) for 48 hours. Western blot analysis of (**A** and **B**). Sp1 (**A** and **C**). MICU1 expression. **A** through **C**, Sp1 (upper bands) and MICU1 (middle bands) were normalized to α-tubulin (lower bands). **D**, Pyruvate dehydrogenase (PDH) enzyme activity was measured in the H9c2 lysates from Scr miR-181c mimic (miR-181c OE) transfected groups treated with/without epicatechin. **P*<0.05, vs Scr, and †*P*<0.05, vs miR-181c OE untreated. n=3 to 5.

miR-181c Regulates (Sp1↓→MICU1↓→$[Ca^{2+}]_m$↑) Pathway Through ROS Production

Overexpression of miR-181c can activate mitochondrial ROS production and increase $[Ca^{2+}]_m$.[19] We have observed a significant increase in mitochondrial ROS production (Figure 5A) and $[Ca^{+2}]_m$ (Figure 5B) when we overexpress miR-181c in NMVM isolated from WT pups. As expected, Mito-TEMPO treatment significantly lowered mitochondrial ROS production in all the groups (Figure 5A). Interestingly, Mito-TEMPO treatment also significantly lowered $[Ca^{+2}]_m$ in miR-181c OE group (Figure 5B). This suggests that the effect of miR-181c on $[Ca^{+2}]_m$ is a downstream effect of ROS.

The Role of Sp1 in Increasing MICU1 Expression in miR-181c/$d^{-/-}$ Mice

181c/$d^{-/-}$ mice are protected from ischemia/reperfusion (I/R) injury,[22] and increased $[Ca^{2+}]_m$ has been shown to be an important determinant of I/R injury.[45,46] We hypothesized that higher MICU1 expression in miR-181c/$d^{-/-}$ hearts inhibits mitochondrial Ca^{2+} uptake under baseline conditions, which might protect the heart from I/R injury (miR-181c↓→mt-COX1↑→ROS↓→Sp1↑→MICU1↑→$[Ca^{2+}]_m$↓→I/R injury↓). Sp1 is a key transcription factor (Figure 1C and 1D) which modulates MICU1 expression in miR-181c/$d^{-/-}$ hearts (Figure 2A and 2B). We have also observed that the activation of Sp1 with epicatechin treatment can overcome the inhibitory effects of miR-181c overexpression and upregulate MICU1 expression (Figure 4A and 4C). To further validate the potential role of Sp1 in miR-181c induced MICU1 regulation, we used small interfering RNA (siRNA) against Sp1 (siSp1) in the NMVM model (Figure 6A). NMVM were isolated from WT and miR-181c/$d^{-/-}$ animals and transfected with either scrambled siRNA or siSp1 for 48 hours. siSp1 transfection significantly lowers Sp1 expression in both WT and miR-181c/$d^{-/-}$ NMVMs (Figure 6B and 6D), without any alteration to mt-COX1 expression (Figure 6B and 6C). Importantly, siSp1 transfection significantly lowers MICU1 expression in miR-181c/$d^{-/-}$ NMVM compared with scrambled siRNA-

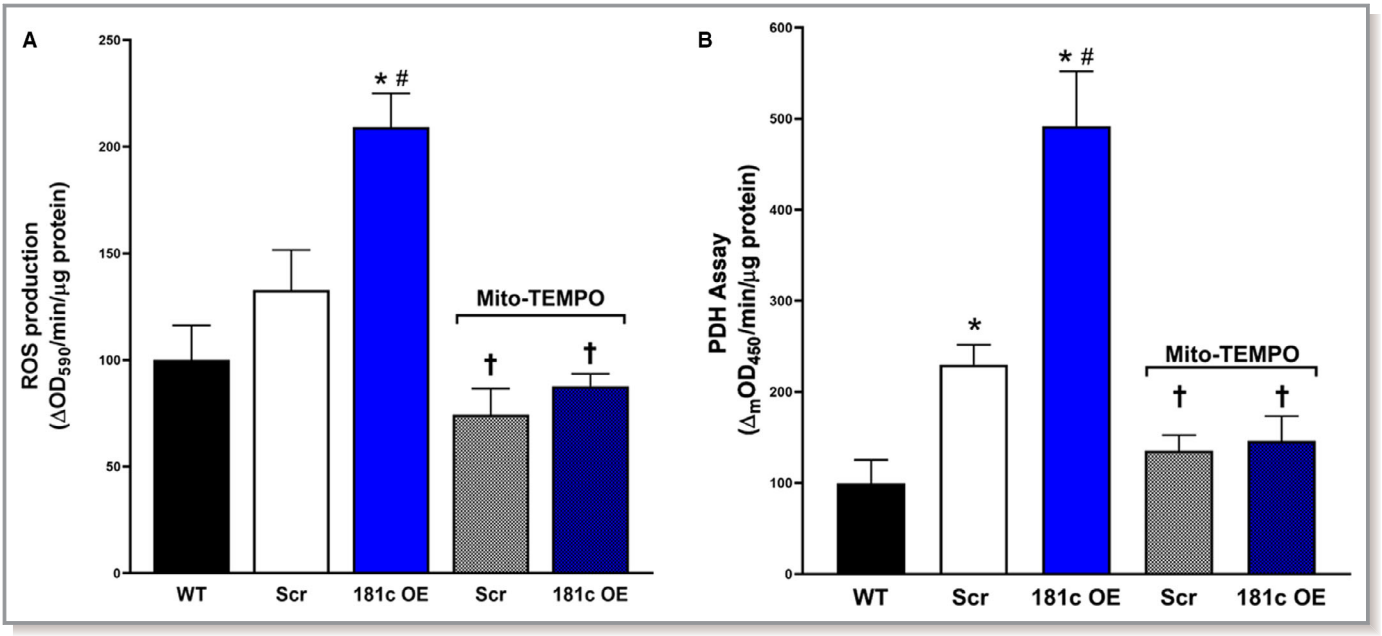

Figure 5. Impact the rate of ROS production in the miR-181c induced mitochondrial Ca^{2+}–entry pathway. NMVMs were isolated from C57BL6 (WT) pups. The NMVMs were then transfected with either scramble sequence (Scr) or miR-181c (miR-181c OE) in the presence or absence of Mito-TEMPO (25 μmol/L) for 48 hours. **A**, Amplex red assay was performed to measure the rate of ROS production and (**B**) the pyruvate dehydrogenase (PDH) activity assay was performed to measure $[Ca^{2+}]_m$. *P<0.05 vs WT and Control (without any transfection; Ctrl.); #P<0.05 vs Scr.; †miR-181c OE without Mito-TEMPO. n=8. NMVMs indicates neonatal mouse ventricular myocytes; ROS, reactive oxygen species; WT, wild-type.

transfected miR-181c/$d^{-/-}$ NMVM (Figure 6B and 6E). These data suggest that mt-COX1 is upstream of Sp1, whereas MICU1 is a downstream target of Sp1. Downregulation of MICU1 due to siSp1 transfection also increases $[Ca^{2+}]_m$ in the miR-181c/$d^{-/-}$ NMVM, as assessed by PDH activity (Figure 6F).

Downregulation MICU1 Does Not Alter Sp1 at Baseline in miR-181c/$d^{-/-}$ Cardiomyocytes

As shown in Figure 6, MICU1 expression can be altered by siSp1. Sp1 is a DNA-binding protein with 3 zinc fingers (Cys2His2–type zinc finger), which are required for recognizing GC-rich promoter sequences.[47,48] Numerous genes have GC-rich promoters. Indeed, it has been shown that Sp1 can bind to several promoter regions of different genes,[49–51] including the SERCA2 gene, an important Ca^{2+} regulatory gene.[52] To focus on the role of MICU1 in $[Ca^{2+}]_m$ regulation in miR-181c/$d^{-/-}$ mice, siRNA against MICU1 (siMICU1) was transfected in the NMVM model (Figure 7A). There were no *significant* effects on mt-COX1 and Sp1 expression with siMICU1 transfection (Figure 7B through 7D). siMICU1 transfection in miR-181c/$d^{-/-}$ and WT NMVMs significantly lowered MICU1 expression (Figure 7E). These data indicate that both mt-COX1 and Sp1 are upstream of MICU1, and downregulation of MICU1 in miR-181c/$d^{-/-}$ NMVM can eliminate the effect on $[Ca^{2+}]_m$. Knocking down MICU1 using siMICU1 transfection increases ROS production in both groups: WT NMVM and the miR-181c/$d^{-/-}$ NMVM, as measured by Amplex red (Figure 7F). However, the level of ROS in the miR-181c/$d^{-/-}$ NMVM is significantly lower in both conditions (with/without siMICU1 transfection) compared with corresponding WT NMVM group (Figure 7F).

Higher MICU1 Expression in miR-181c/$d^{-/-}$ Confers Cardioprotection

miR-181c/$d^{-/-}$ hearts are protected during 20 minutes global ischemia followed by 2 hours reperfusion.[22] $[Ca^{2+}]_m$ overload has been shown to cause I/R injury.[45,46] Therefore, we hypothesized that lower $[Ca^{2+}]_m$ due to higher expression of MICU1 under low $[Ca^{2+}]_{cyto}$ conditions in 181c/$d^{-/-}$ mice can protect the heart from I/R injury. To illustrate this, we used short-hairpin RNA against MICU1 (shMICU1), packaged in lentivirus (lenti-shMICU1). We injected, through the jugular vein, 10^6 viral particles/injection, of either lenti-shScramble or lenti-shMICU1, into miR-181c/$d^{-/-}$ and WT mice. In vivo delivery of lenti-shMICU1 can decrease MICU1 expression in the heart by almost 40% in both groups of mice. Consistent with our previous studies, we have identified a significant upregulation of mt-COX1, Sp1, and MICU1 in the miR-181c/$d^{-/-}$ animals compared with WT littermates (Figure 8A and

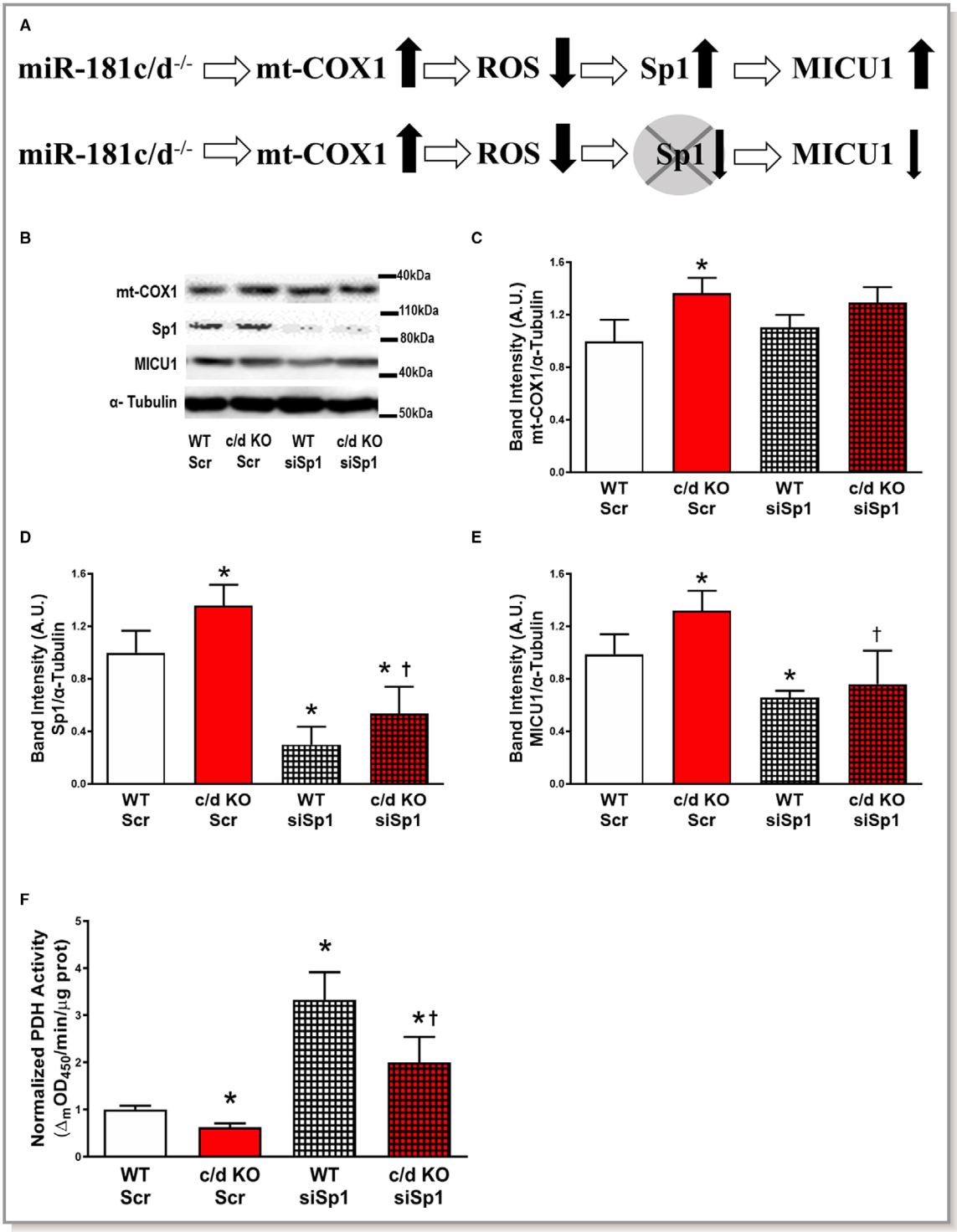

Figure 6. miR-181c effect on mitochondrial Ca^{2+} entry can be intervene by altering Sp1 expression. **A**, Primary NMVMs were isolated from WT (C57BL6/j) and miR-181c/d$^{-/-}$ (c/d KO) pup hearts. Sp1 expression was altered with siRNA against Sp1 (siSp1). Western blot analysis (**B** and **C**). mt-COX1, (**B** and **D**). Sp1, and (**B** and **E**). MICU1 expression. **B** through **E**, mt-COX1 (upper bands), Sp1 (second from the top bands) and MICU1 (third from the top bands) were normalized to α-tubulin (lower bands). **F**, Pyruvate dehydrogenase (PDH) enzyme activity was measured in the primary NMVM lysates from WT or miR-181c/d$^{-/-}$ groups transfected with either scramble-sequence (Scr) or siSp1 for 48 hours. *P<0.05, vs WT Scr, and $^{\dagger}P$<0.05, vs c/d KO Scr. n=3 to 5. KO indicates knockout; NMVMs indicates neonatal mouse ventricular myocytes; Sp1, specificity protein; WT, wild-type.

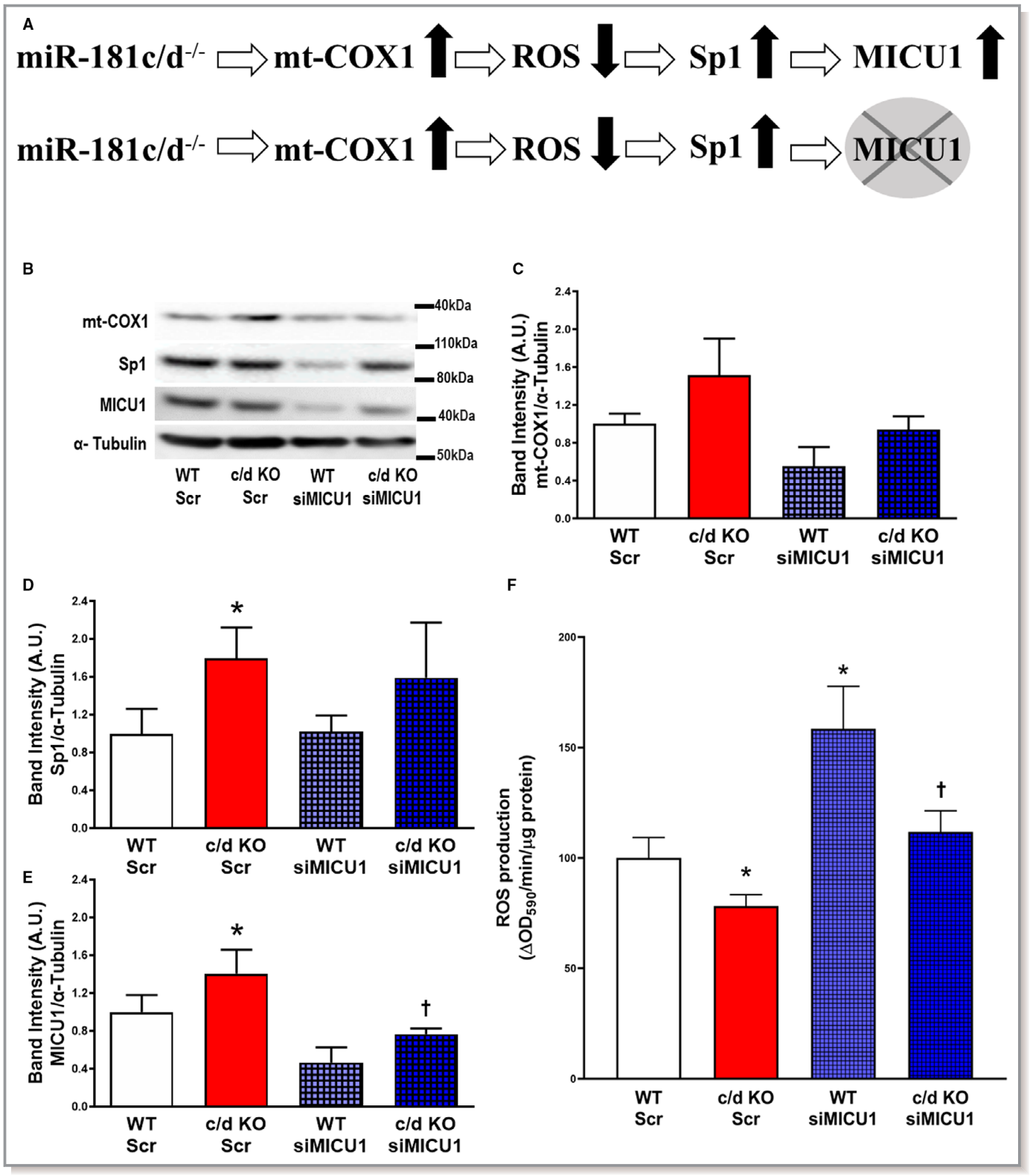

Figure 7. miR-181c alters MICU1 expression through Sp1 alteration. **A**, Primary NMVMs were isolated from WT (C57BL6/j) and miR-181c/$d^{-/-}$ (c/d KO) pup hearts. MICU1 expression was altered with small interfering RNA against MICU1 (siMICU1). Western blot analysis (**B** and **C**). mt-COX1, (**B** and **D**). Sp1, and (**B** and **E**). MICU1 expression. **B** through **E**, mt-COX1 (upper bands), Sp1 (second from the top bands) and MICU1 (third from the top bands) were normalized to α-tubulin (lower bands). **F**, Amplex red assay was performed to measure the rate of ROS production from the isolated NMVMs with/without siMICU1 transfection. **P*<0.05, vs WT Scr, and †*P*<0.05, vs c/d KO Scr. n=3 to 5. KO indicates knockout; NMVMs indicates neonatal mouse ventricular myocytes; ROS, reactive oxygen species; Sp1, specificity protein; WT, wild-type.

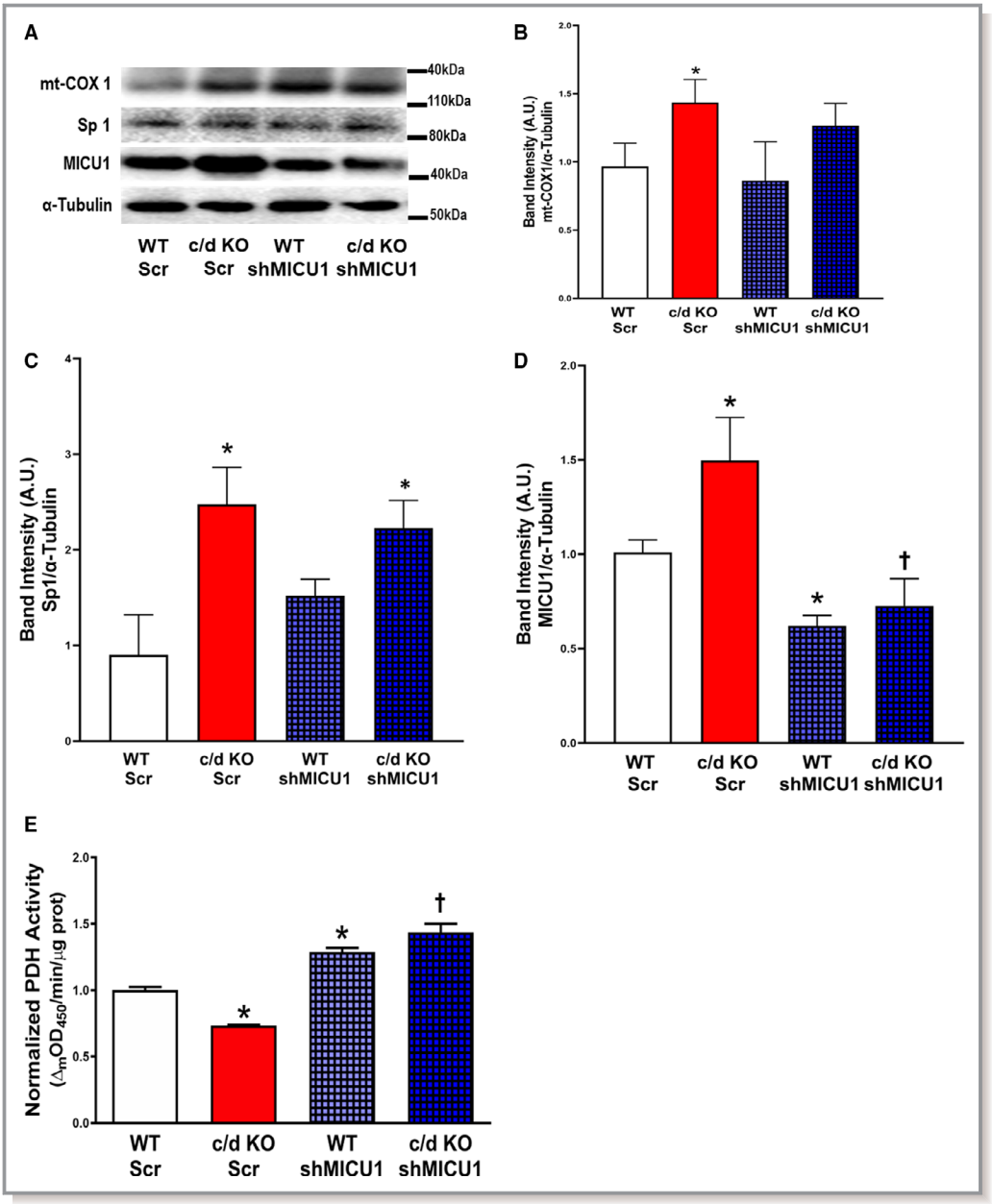

Figure 8. Role of miR-181c on mitochondrial Ca^{2+}-entry through MICU1, in vivo. Total heart homogenates were prepared from miR-181c/$d^{-/-}$ (c/d KO) and corresponding WT (C57BL6/j) with lentivirus treatment. Lentivirus was either packaged with short-hairpin RNA against MICU1 (shMICU1) or scramble sequence (Scr) as a control. **A** through **D**, Immunoblots were probed with mt-COX1, Sp1, and MICU1 antibodies. **B** through **D**, Densitometry was performed after developing the western blots. **E**, Pyruvate dehydrogenase (PDH) enzyme activity was measured in the whole heart homogenate from WT or (c/d KO) hearts injected with either scramble-sequence (Scr) or shMICU1 at the baseline condition (low $[Ca^{2+}]_{cyto}$). **P*<0.05, vs WT Scr, and †*P*<0.05, vs c/d KO Scr. n=6. KO indicates knockout; NMVMs indicates neonatal mouse ventricular myocytes; Sp1, specificity protein; WT, wild-type.

8B). Lenti-shMICU1 did not alter the expression of mt-COX1 or Sp1 in either the WT or c/d knockout groups (WT Scramble versus WT shMICU1 and c/d knockout Scramble versus c/d knockout shMICU1) (Figure 8A and 8B). In accordance with our in vitro data (Figure 7), in vivo data again suggest that mt-COX1 and Sp1 are upstream of MICU1. Figure 8E also shows that lenti-shMICU1 treatment eliminates the protective effects against $[Ca^{2+}]_m$ overload in miR-181c/$d^{-/-}$ hearts. We also perfused isolated hearts after either lenti-shScramble or lenti-shMICU1 treatment in both miR-181c/$d^{-/-}$ and WT mice. Figure 9A and 9B show that following lenti-shMICU1 treatment, cardioprotection from I/R injury in miR-181c/$d^{-/-}$

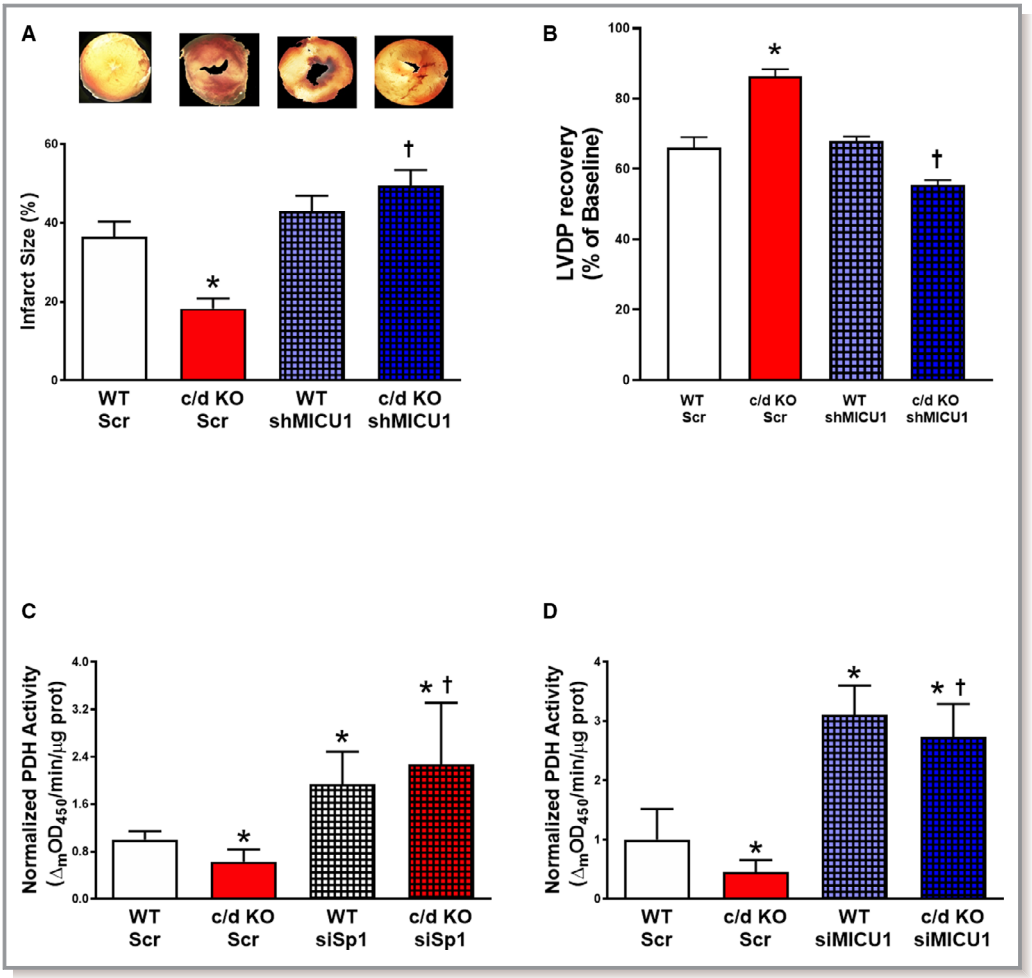

Figure 9. Cardioprotective effect of miR-181c/d$^{-/-}$ from ischemia/reperfusion injury is through Sp1→MICU1 signaling pathway. Langendorff model was used to induce ischemia/reperfusion (I/R) injury to the mice heart. **A**, Infarct size and (**B**) left ventricular diastolic pressure (LVDP) recovery was calculated after 20 minutes of global ischemia, followed by 2 hours of reperfusion from 4 groups of mice: C57BL6/j (WT) injected with Scramble sequence (Scr), miR-181c/d$^{-/-}$ (c/d KO) with Scr, WT with short-hairpin (sh) MICU1, and c/d KO with shMICU1. Primary NMVMs were isolated from either WT or c/d KO mouse pup hearts. These isolated NMVMs were transfected with either scramble sequence or (**C**) siRNA against Sp1 or (**D**) siRNA against MICU1. Pyruvate dehydrogenase enzyme activity (PDH, normalized to WT-Scr) was measured in the NMVM lysates after coverslip-induced ischemia from 4 groups: (**C**) WT transfected with Scr, c/d KO with Scr, WT with small interfering (si)Sp1, and c/d KO with siSp1. **D**, WT transfected with Scr, c/d KO with Scr, WT with siMICU1, and c/d KO with siMICU1. *P<0.05, vs WT Scr, and $^{\dagger}P$<0.05, vs c/d KO Scr. n=5. KO indicates knockout; NMVMs indicates neonatal mouse ventricular myocytes; Sp1, specificity protein; WT, wild-type.

mice is lost, suggesting a pivotal role for higher MICU1 expression in I/R injury.

To further validate the pathway whereby lowering miR-181c up-regulates MICU1 expression in the heart, we used the NMVM monolayer I/R model.[53] To examine our hypothesis that the protection from I/R-injury in miR-181c/d$^{-/-}$ NMVM is due to inhibiting $[Ca^{2+}]_m$ entry from increased MICU1 expression (through increased mt-COX1→Sp1 signaling), we used siRNAs against (1) Sp1 and (2) MICU1. NMVM from both WT and miR-181c/d$^{-/-}$ groups were transfected with either scrambled siRNA or one of the two siRNAs. 48 hours after transfection, PDH activity was measured after 30 minutes ischemia followed by 15 minutes reperfusion by lysing the NMVM monolayer (Figure 9C and 9D). PDH activity (used as a surrogate for $[Ca^{2+}]_m$) is significantly lower in the NMVMs from the miR-181c/d$^{-/-}$ group compared with WT immediately after I/R injury (Figure 9C and 9D, white versus red bar). Moreover, if we knock-down either Sp1 or MICU1 in the NMVM in both groups (WT and miR-181c/d$^{-/-}$) using siSp1 (Figure 9C) or siMICU1 (Figure 9D), respectively, we

observe a significantly higher PDH activity in the miR-181c/$d^{-/-}$ NMVM monolayer compared with the control (Figure 9C and 9D). Interestingly, there is no statistically significant difference between WT and miR-181c/$d^{-/-}$ treated either with siSp1 or with siMICU1 (Figure 9C and 9D). These data further support the hypothesis that the loss of miR-181c protects the heart from I/R injury through the mt-COX1→ROS→Sp1→MICU1 signaling pathway.

Discussion

The importance of MCU and its regulatory proteins in cellular function and survival has been well established through the use of genetically altered in vitro/in vivo models.[4–9] However, the role of changes in MCU regulatory proteins in pathophysiological processes is not completely known. In this study, we report on a novel signaling pathway that is initiated by a change in expression of a single microRNA, which impacts 1 respiratory chain component, and subsequently leads to a change in expression of a key regulatory component of MCU, MICU1. The findings of this study highlight the interactive and bidirectional communication between mitochondria and nucleus and how this communication plays a significant role in the pathophysiology of cardiac health. Mitochondria-nuclear communication is essential for cardiomyocyte function; the activation of miR-181c expression perturb the mitochondria-nuclear communication. Identifying this novel signaling pathway involving miR-181c→mt-COX1→ROS→Sp1→MICU1 to combat I/R injury in the heart focuses attention on miR-181c as a candidate therapeutic target. As it has already been established that miR-181c is a "druggable" target,[22] these findings identify a paradigm useful for testing the efficacy of miR-181c antagomiRs in acute myocardial infarction. From a broader perspective, these data highlight the potential for developing strategies to inhibit increases in $[Ca^{2+}]_m$ that may lead to myocardial injury, and these findings provide proof-of-principle that targeting miR-181c pathways can be effective.

The nuclear-encoded miR-181 family members play an important role in cardiac function by regulating target genes in both the cytoplasm and the mitochondria. miR-181a/b regulates PTEN expression in the cytoplasm, whereas miR-181c regulates the mitochondrial gene mt-COX1 in the mitochondria.[22] Particularly in cardiomyocytes, there is no cytosolic mRNA target for miR-181c. The lack of a thermodynamically stable RISC in the cytoplasm favors the translocation of the Ago2/miR-181c complex into the mitochondria. As miR-181c could form a stable Ago2/mt-COX1/miR-181c complex in the mitochondria, miR-181c can primarily localize in the mitochondria of the cardiomyocytes. A pivotal role for mitochondrial miR-181c in cardiac dysfunction has been previously demonstrated both in vitro[20] and in vivo.[19] We[19,20,22] and others[54] have identified a significant role for miR-181 in the heart during end-stage heart failure. After maturing via conventional miRNA machineries in the cytoplasm, mature miR-181c translocates into the mitochondrial compartment.[26] miR-181c mainly localizes to mitochondria in cardiomyocytes.[20] There are several physiological conditions where mitochondrial ROS levels change in the heart. One of such physiological condition is a sex difference. Our group has demonstrated that ROS production in the pre-menopausal female heart is significantly lower compared with the age-matched male heart.[55] Therefore, we hypothesized that the endogenous level of miR-181c would be less compared with age-matched male hearts. Figure S4 shows a significant decrease in miR-181c expression in the female hearts compared with male hearts. Chronic overexpression of miR-181c can cause elevated ROS production, higher $[Ca^{2+}]_m$ levels, and altered mitochondrial function, which ultimately leads to cardiac dysfunction.[19] The coordinated genetic regulation between mitochondria and nucleus that regulates $[Ca^{2+}]_m$ was not recognized previously; however, this current study has established a novel pathway whereby lowering miR-181c protects the heart from I/R injury by increasing MICU1 and attenuating the rise in $[Ca^{2+}]_m$.

Ca^{2+} is a key regulator of mitochondrial function. Increased $[Ca^{2+}]_m$ has been shown to be an important regulator of mitochondrial function by activating mPTP.[1,2] The MCU forms a complex with several regulatory proteins (MCUR1, EMRE, MICU1, and MICU2), and the mitochondrial membrane potential ($\Delta\Psi_m$) drives $[Ca^{2+}]_m$ entry through the MCU channel.[4–9] MCU and its regulatory proteins form a complex network to set $[Ca^{2+}]_m$. As mitochondrial function changes, multiple cellular and physiological processes are affected, contributing to the development of various diseases.[45,46] $[Ca^{2+}]_m$ overload plays an important role in the pathogenesis of heart disease, such as I/R injury.[45,46] Thus, modulating $[Ca^{2+}]_m$ entry can determine the fate of cardiomyocytes during periods of I/R.

In summary, these studies demonstrate, for the first time, the potential physiologic/pathophysiologic role for miR-181c in $[Ca^{2+}]_m$ entry via regulating MICU1 expression in the heart. Additionally, our findings establish miR-181c as a potential therapeutic target in various cardiovascular diseases, such as I/R injury.

Acknowledgments

Author contributions: Drs O'Rourke, Kohr, Murphy, Steenbergen, and Das designed the experiments. Dr Banavath, Dr Roman, Mr Mackowski, Mr Biswas, Dr Nomura, Dr Solhjoo, and Dr Afzal carried out most of the experiments. Drs O'Rourke, Kohr, Murphy, Steenbergen, and Das wrote the article.

Sources of Funding

This work was supported by grants from the AHA, 14SDG18890049 and Seed Grants on Sex/Gender Differences in Medicine and Public Health (Das), 14POST20000018 and 5T32HL007227 (Solhjoo), and the NIH 5R01HL039752 (Steenbergen), R01HL137259 (O'Rourke), and R01HL136496 (Kohr).

Disclosures

None.

References

1. Glancy B, Balaban RS. Role of mitochondrial Ca^{2+} in the regulation of cellular energetics. *Biochemistry*. 2012;51:2959–2973.
2. Liu T, O'Rourke B. Regulation of mitochondrial Ca^{2+} and its effects on energetics and redox balance in normal and failing heart. *J Bioenerg Biomembr*. 2009;41:127–132.
3. Brookes PS, Yoon Y, Robotham JL, Anders MW, Sheu SS. Calcium, ATP, and ROS: a mitochondrial love-hate triangle. *Am J Physiol Cell Physiol*. 2004;287: C817–C833.
4. Kwong JQ, Lu X, Correll RN, Schwanekamp JA, Vagnozzi RJ, Sargent MA, York AJ, Zhang J, Bers DM, Molkentin JD. The mitochondrial calcium uniporter selectively matches metabolic output to acute contractile stress in the heart. *Cell Rep*. 2015;12:15–22.
5. Vais H, Mallilankaraman K, Mak DD, Hoff H, Payne R, Tanis JE, Foskett JK. EMRE is a matrix Ca(2+) sensor that governs gatekeeping of the mitochondrial Ca(2+) uniporter. *Cell Rep*. 2016;14:403–410.
6. De Stefani D, Patron M, Rizzuto R. Structure and function of the mitochondrial calcium uniporter complex. *Biochim Biophys Acta*. 2015;1853: 2006–2011.
7. Hoffman NE, Chandramoorthy HC, Shamugapriya S, Zhang X, Rajan S, Mallilankaraman K, Gandhirajan RK, Vagnozzi RJ, Ferrer LM, Sreekrishnanilayam K, Natarajaseenivasan K, Vallem S, Force T, Choi ET, Cheung JY, Madesh M. MICU1 motifs define mitochondrial calcium uniporter binding and activity. *Cell Rep*. 2013;5:1576–1588.
8. Sancak Y, Markhard AL, Kitami T, Kovacs-Bogdan E, Kamer KJ, Udeshi ND, Carr SA, Chaudhuri D, Clapham DE, Li AA, Calvo SE, Goldberger O, Mootha VK. EMRE is an essential component of the mitochondrial calcium uniporter complex. *Science*. 2013;342:1379–1382.
9. Mallilankaraman K, Doonan P, Cardenas C, Chandramoorthy HC, Muller M, Miller R, Hoffman NE, Gandhirajan RK, Molgo J, Birnbaum MJ, Rothberg BS, Mak DO, Foskett JK, Madesh M. MICU1 is an essential gatekeeper for MCU-mediated mitochondrial Ca(2+) uptake that regulates cell survival. *Cell*. 2012;151:630–644.
10. Bagur R, Hajnoczky G. Intracellular Ca(2+) sensing: its role in calcium homeostasis and signaling. *Mol Cell*. 2017;66:780–788.
11. Paillard M, Csordas G, Szanda G, Golenar T, Debattisti V, Bartok A, Wang N, Moffat C, Seifert EL, Spat A, Hajnoczky G. Tissue-specific mitochondrial decoding of cytoplasmic Ca(2+) signals is controlled by the stoichiometry of MICU1/2 and MCU. *Cell Rep*. 2017;18:2291–2300.
12. Baughman JM, Perocchi F, Girgis HS, Plovanich M, Belcher-Timme CA, Sancak Y, Bao XR, Strittmatter L, Goldberger O, Bogorad RL, Koteliansky V, Mootha VK. Integrative genomics identifies MCU as an essential component of the mitochondrial calcium uniporter. *Nature*. 2011;476:341–345.
13. Perocchi F, Gohil VM, Girgis HS, Bao XR, McCombs JE, Palmer AE, Mootha VK. MICU1 encodes a mitochondrial EF hand protein required for Ca(2+) uptake. *Nature*. 2010;467:291–296.
14. Csordas G, Golenar T, Seifert EL, Kamer KJ, Sancak Y, Perocchi F, Moffat C, Weaver D, de la Fuente Perez S, Bogorad R, Koteliansky V, Adijanto J, Mootha VK, Hajnoczky G. MICU1 controls both the threshold and cooperative activation of the mitochondrial Ca(2)(+) uniporter. *Cell Metab*. 2013;17:976–987.
15. Kamer KJ, Mootha VK. MICU1 and MICU2 play nonredundant roles in the regulation of the mitochondrial calcium uniporter. *EMBO Rep*. 2014;15: 299–307.
16. Patron M, Checchetto V, Raffaello A, Teardo E, Vecellio Reane D, Mantoan M, Granatiero V, Szabo I, De Stefani D, Rizzuto R. MICU1 and MICU2 finely tune the mitochondrial Ca^{2+} uniporter by exerting opposite effects on MCU activity. *Mol Cell*. 2014;53:726–737.
17. de la Fuente S, Matesanz-Isabel J, Fonteriz RI, Montero M, Alvarez J. Dynamics of mitochondrial Ca^{2+} uptake in MICU1-knockdown cells. *Biochem J*. 2014;458:33–40.
18. Liu JC, Liu J, Holmstrom KM, Menazza S, Parks RJ, Fergusson MM, Yu ZX, Springer DA, Halsey C, Liu C, Murphy E, Finkel T. MICU1 serves as a molecular gatekeeper to prevent in vivo mitochondrial calcium overload. *Cell Rep*. 2016;16:1561–1573.
19. Das S, Bedja D, Campbell N, Dunkerly B, Chenna V, Maitra A, Steenbergen C. miR-181c regulates the mitochondrial genome, bioenergetics, and propensity for heart failure in vivo. *PLoS One*. 2014;9:e96820.
20. Das S, Ferlito M, Kent OA, Fox-Talbot K, Wang R, Liu D, Raghavachari N, Yang Y, Wheelan SJ, Murphy E, Steenbergen C. Nuclear miRNA regulates the mitochondrial genome in the heart. *Circ Res*. 2012;110:1596–1603.
21. Jung KA, Lee S, Kwak MK. NFE2L2/NRF2 activity is linked to mitochondria and AMP-activated protein kinase signaling in cancers through miR-181c/mitochondria-encoded cytochrome c oxidase regulation. *Antioxid Redox Signal*. 2017;27:945–961.
22. Das S, Kohr M, Dunkerly-Eyring B, Lee DI, Bedja D, Kent OA, Leung AK, Henao-Mejia J, Flavell RA, Steenbergen C. Divergent effects of miR-181 family members on myocardial function through protective cytosolic and detrimental mitochondrial microRNA targets. *J Am Heart Assoc*. 2017;6:e004694. DOI: 10.1161/JAHA.116.004694.
23. Dasgupta N, Peng Y, Tan Z, Ciraolo G, Wang D, Li R. miRNAs in mtDNA-less cell mitochondria. *Cell Death Discov*. 2015;1:15004.
24. Suzuki T, Yamamoto M. Stress-sensing mechanisms and the physiological roles of the Keap1-Nrf2 system during cellular stress. *J Biol Chem*. 2017;292:16817–16824.
25. Das S, Wong R, Rajapakse N, Murphy E, Steenbergen C. Glycogen synthase kinase 3 inhibition slows mitochondrial adenine nucleotide transport and regulates voltage-dependent anion channel phosphorylation. *Circ Res*. 2008;103:983–991.
26. Macgregor-Das AM, Das S. A microRNA's journey to the center of the mitochondria. *Am J Physiol Heart Circ Physiol*. 2018;315:H206–H215.
27. Martin M. Cutadapt removes adapter sequence from high-throughput sequencing reads. *EMBnet J*. 2011;17:10–12.
28. Dobin A, Davis CA, Schlesinger F, Drenkow J, Zaleski C, Jha S, Batut P, Chaisson M, Gingeras TR. STAR: ultrafast universal RNA-seq aligner. *Bioinformatics*. 2013;29:15–21.
29. Liao Y, Smyth GK, Shi W. FeatureCounts: an efficient general purpose program for assigning sequence reads to genomic features. *Bioinformatics*. 2014;30:923–930.
30. Harrow J, Frankish A, Gonzalez JM, Tapanari E, Diekhans M, Kokocinski F, Aken BL, Barrell D, Zadissa A, Searle S, Barnes I, Bignell A, Boychenko V, Hunt T, Kay M, Mukherjee G, Rajan J, Despacio-Reyes G, Saunders G, Steward C, Harte R, Lin M, Howald C, Tanzer A, Derrien T, Chrast J, Walters N, Balasubramanian S, Pei B, Tress M, Rodriguez JM, Ezkurdia I, van Baren J, Brent M, Haussler D, Kellis M, Valencia A, Reymond A, Gerstein M, Guigo R, Hubbard TJ. GENCODE: the reference human genome annotation for the ENCODE Project. *Genome Res*. 2012;22:1760–1774.
31. Smyth G, Gentleman R, Carey V, Dudoit S, Irizarry R, Huber W. Limma: Linear models for microarray data. *Bioinformatics and Computational Biology Solutions Using R and Bioconductor*. 2005:397–420.
32. Ritchie ME, Phipson B, Wu D, Hu Y, Law CW, Shi W, Smyth GK. Limma powers differential expression analyses for RNA-sequencing and microarray studies. *Nucleic Acids Res*. 2015;43:e47.
33. Robinson MD, Oshlack A. A scaling normalization method for differential expression analysis of RNA-seq data. *Genome Biol*. 2010;11:R25.
34. Madar V, Batista S. FastLSU: a more practical approach for the Benjamini-Hochberg FDR controlling procedure for huge-scale testing problems. *Bioinformatics*. 2016;32:1716–1723.
35. Luo W, Friedman MS, Shedden K, Hankenson KD, Woolf PJ. GAGE: generally applicable gene set enrichment for pathway analysis. *BMC Bioinformatics*. 2009;10:161.
36. Schafer G, Cramer T, Suske G, Kemmner W, Wiedenmann B, Hocker M. Oxidative stress regulates vascular endothelial growth factor-A gene transcription through Sp1- and Sp3-dependent activation of two proximal GC-rich promoter elements. *J Biol Chem*. 2003;278:8190–8198.
37. Morel Y, Barouki R. Repression of gene expression by oxidative stress. *Biochem J*. 1999;342(Pt 3):481–496.
38. Ushio-Fukai M, Nakamura Y. Reactive oxygen species and angiogenesis: NADPH oxidase as target for cancer therapy. *Cancer Lett*. 2008;266: 37–52.

39. Ji L, Liu F, Jing Z, Huang Q, Zhao Y, Cao H, Li J, Yin C, Xing J, Li F. MICU1 alleviates diabetic cardiomyopathy through mitochondrial Ca(2+)-dependent antioxidant response. *Diabetes*. 2017;66:1586–1600.

40. Rasmussen TP, Wu Y, Joiner ML, Koval OM, Wilson NR, Luczak ED, Wang Q, Chen B, Gao Z, Zhu Z, Wagner BA, Soto J, McCormick ML, Kutschke W, Weiss RM, Yu L, Boudreau RL, Abel ED, Zhan F, Spitz DR, Buettner GR, Song LS, Zingman LV, Anderson ME. Inhibition of MCU forces extramitochondrial adaptations governing physiological and pathological stress responses in heart. *Proc Natl Acad Sci USA*. 2015;112:9129–9134.

41. van der Veen JN, Lingrell S, da Silva RP, Jacobs RL, Vance DE. The concentration of phosphatidylethanolamine in mitochondria can modulate ATP production and glucose metabolism in mice. *Diabetes*. 2014;63:2620–2630.

42. Shanmughapriya S, Rajan S, Hoffman NE, Zhang X, Guo S, Kolesar JE, Hines KJ, Ragheb J, Jog NR, Caricchio R, Baba Y, Zhou Y, Kaufman BA, Cheung JY, Kurosaki T, Gill DL, Madesh M. Ca^{2+} signals regulate mitochondrial metabolism by stimulating CREB-mediated expression of the mitochondrial Ca^{2+} uniporter gene MCU. *Sci Signal*. 2015;8:ra23.

43. Luongo TS, Lambert JP, Yuan A, Zhang X, Gross P, Song J, Shanmughapriya S, Gao E, Jain M, Houser SR, Koch WJ, Cheung JY, Madesh M, Elrod JW. The mitochondrial calcium uniporter matches energetic supply with cardiac workload during stress and modulates permeability transition. *Cell Rep*. 2015;12:23–34.

44. Dong ZX, Wan L, Wang RJ, Shi YQ, Liu GZ, Zheng SJ, Hou HL, Han W, Hai X. (-)-Epicatechin suppresses angiotensin II-induced cardiac hypertrophy via the activation of the SP1/SIRT1 signaling pathway. *Cell Physiol Biochem*. 2017;41:2004–2015.

45. Murphy E, Steenbergen C. Did a classic preconditioning study provide a clue to the identity of the mitochondrial permeability transition pore? *Circ Res*. 2013;113:852–855.

46. Murphy E, Steenbergen C. Mechanisms underlying acute protection from cardiac ischemia-reperfusion injury. *Physiol Rev*. 2008;88:581–609.

47. Briggs MR, Kadonaga JT, Bell SP, Tjian R. Purification and biochemical characterization of the promoter-specific transcription factor, Sp1. *Science*. 1986;234:47–52.

48. Kadonaga JT, Courey AJ, Ladika J, Tjian R. Distinct regions of Sp1 modulate DNA binding and transcriptional activation. *Science*. 1988;242:1566–1570.

49. Johar K, Priya A, Dhar S, Liu Q, Wong-Riley MT. Neuron-specific specificity protein 4 bigenomically regulates the transcription of all mitochondria- and nucleus-encoded cytochrome c oxidase subunit genes in neurons. *J Neurochem*. 2013;127:496–508.

50. Lu J, Wang K, Rodova M, Esteves R, Berry D, E L, Crafter A, Barrett M, Cardoso SM, Onyango I, Parker WD, Fontes J, Burns JM, Swerdlow RH. Polymorphic variation in cytochrome oxidase subunit genes. *J Alzheimers Dis*. 2010;21:141–154.

51. Jimenez-Gutierrez LR, Hernandez-Lopez J, Islas-Osuna MA, Muhlia-Almazan A. Three nucleus-encoded subunits of mitochondrial cytochrome c oxidase of the whiteleg shrimp *Litopenaeus vannamei*: cDNA characterization, phylogeny and mRNA expression during hypoxia and reoxygenation. *Comp Biochem Physiol B Biochem Mol Biol*. 2013;166:30–39.

52. Koitabashi N, Arai M, Tomaru K, Takizawa T, Watanabe A, Niwano K, Yokoyama T, Wuytack F, Periasamy M, Nagai R, Kurabayashi M. Carvedilol effectively blocks oxidative stress-mediated downregulation of sarcoplasmic reticulum Ca^{2+}-ATPase 2 gene transcription through modification of Sp1 binding. *Biochem Biophys Res Commun*. 2005;328:116–124.

53. Solhjoo S, O'Rourke B. Mitochondrial instability during regional ischemia-reperfusion underlies arrhythmias in monolayers of cardiomyocytes. *J Mol Cell Cardiol*. 2015;78:90–99.

54. Li J, Cao Y, Ma XJ, Wang HJ, Zhang J, Luo X, Chen W, Wu Y, Meng Y, Zhang J, Yuan Y, Ma D, Huang GY. Roles of miR-1-1 and miR-181c in ventricular septal defects. *Int J Cardiol*. 2013;168:1441–1446.

55. Lagranha CJ, Deschamps A, Aponte A, Steenbergen C, Murphy E. Sex differences in the phosphorylation of mitochondrial proteins result in reduced production of reactive oxygen species and cardioprotection in females. *Circ Res*. 2010;106:1681–1691.

SUPPLEMENTAL MATERIAL

Figure S1. shMICU1-lenti efficiency to knock-down MICU1 in NMVMs.

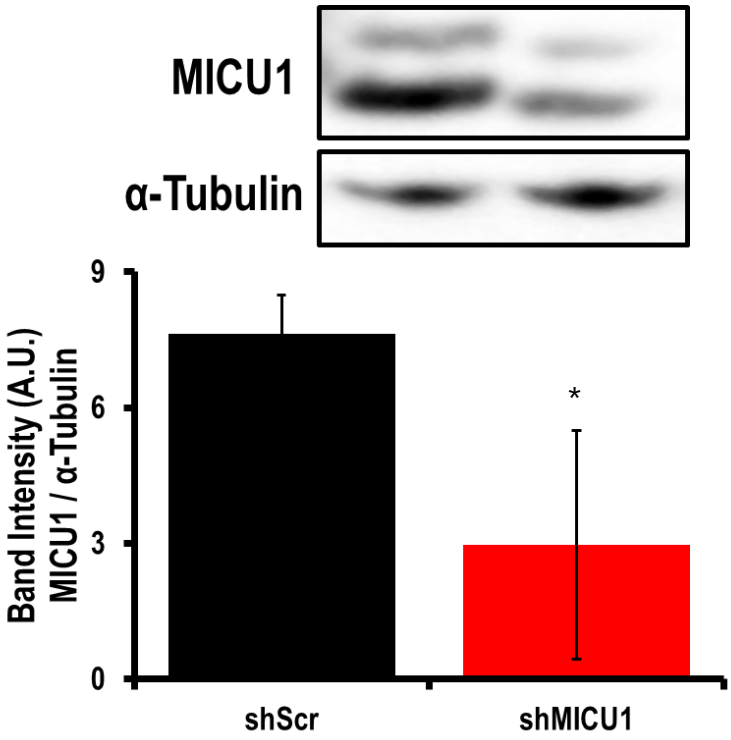

Western blot analysis of Mitochondrial calcium uptake 1 (MICU1) protein in NMVMs from the WT (C57BL/6) pups. **(A)** MICU1 (upper bands) expression was normalized to α-tubulin (lower bands). **(B)** Bar graphs show the quantification of protein expression. Protein lysate was prepared from the virus transfected NMVMs. *p<0.05 vs. WT (n=3).

(A)

```
   1 TTGGCTTGGT TTTTCAGACA GGATCTTATA GAGCCCACAC TAGCCTCAAA CTCACTATGT
  61 AACTAAGTAT GGCTTTGAAC TCCTGATCCT ACTGCCTCTA TCTCTCAGAT TCTGGGATTA
 121 CAGTTCTATG CCACCACATC TGGCTGAAAA TTTTATTCAA CAATTTATAT ATTGATGATT
 181 TTTTTTCTCT TTTCCTTATT CAAATAAAGA GTTAATTTAT CCCGTGAGCC TCCAAAGTGT
 241 TCTATGGTAT TTACGATGCA ATGTGAAATT TACAAGTTTC AGAGATAACA AGATGTGTGT
 301 CCCAAGAGAA GACTTTTATT CGCTCTTTTC TCCTTCCCTT TTTTCATGTA TGTATGTATG
 361 TATGTATGTA TGTATGTATG TATGCATGCA GGTATGTGTG TTCCGCAGCA TGGTTCTGAA
 421 GGTTAGGAGA CAACTTGCAT CAGTCAGTTC TCTCCTTCCA CCATAAGTGT CCTGGGACTC
 481 AAATACGGGT TATCTGGTTT GGTAGTAAGA GCCCTTACCT GCTGAGCTCC TCTGTTTCAT
 541 AATTTGACAC AGGTCTAAGT AAACCACACT AGCCTCTAAG TTCCAAGTGT TGGGAGACTA
 601 GCGGGGACTT CCTGGAAGGA GTGAACGTGG AGAACTGGAG GTGGATAAGA TTAAGATACA
 661 TTATATCTTA CGAAACTGTC AAAGAATAAA TAAAAGATGT TCCTAAAATA AAACCAGTGT
 721 GAGCCTCTAG ACTGGTGGGA AGAACCTCGT TATCAATTTC CCACTTACGG AAGAGCAGGG
 781 TTTAACTAGA AAGAGGCACA GGAGAGGTGG ACTTTGACAG CAGAGAAACA AAATCAGCAA
 841 TGGAATGCAG GAGGGATTTT GCAAATCTGC CGGCATTCCC GCCTAAACAG CGAGGGCGTG
 901 GCACCGACGT GTGGGCGGGG CTGAGGACAG GGCGGGCCCC CAGGCGAGGG CGGAGTCTTG
 961 ACTCGGGGCG GGATCCGAAG TGTGGGCGGG CCCCAGAGAA GGGCGGGGTT GCCTCTCCGC
                                          Sp 1

1021 CCCGCCCCAT TTTCCCCAAC TCGGTTCCTC CCTGCTACGT TTCATCAAGA TCCCGGCAGG
1081 CCCAGCGGCT AAGGGAGTCA CGTGAGAGTG GGCGGAGGAC GCAGAGCGGG GCTCCCCGGC
1141 ATTTGCGTCT CTATGGTTGT CAGAGGTGGG CGGCATTCTC CGAGTTGCTG CTAAAGCTGG
```

(B)

Gene	Species	TF Name	Start	End	Anchor	GC box	Matrix sum.	P VALUE
MICU1	Mus Musculus	GC-Box factors Sp1/GC (+ ve strand)	996	1012	1004	gagaaGGGCgggggttgc	0.951	0.139251

Figure S2. ***In silico*** **analysis of potential binding site of Sp1 on MICU1 promoter. (A)** Promoter region sequence of MICU1 where GC-box region is highlighted in red. **(B)** Statistical confidence calculation for Sp1 to bind to the highlighted GC-box region.

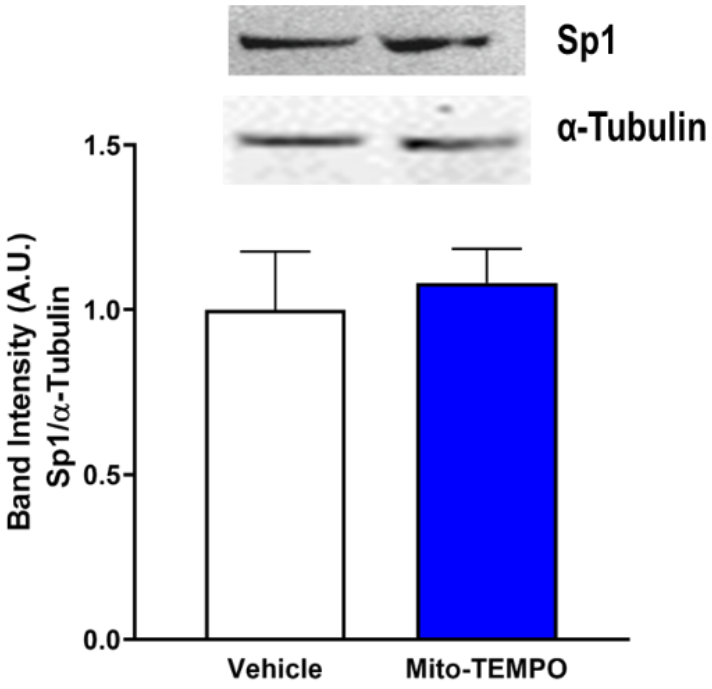

Figure S3. Effect of antioxidant on Sp1 expression. Western blot analysis of Specificity protein 1 protein (Sp1) in H9c2 cell with/without Mito-TEMPO treatment (25 nM for 48 hr). Sp1 (upper bands) expression was normalized to α-tubulin (lower bands). Bar graphs show the quantification of protein expression. Protein lysate was prepared from the H9c2 cell lysate. *p<0.05 vs. WT (n=5).

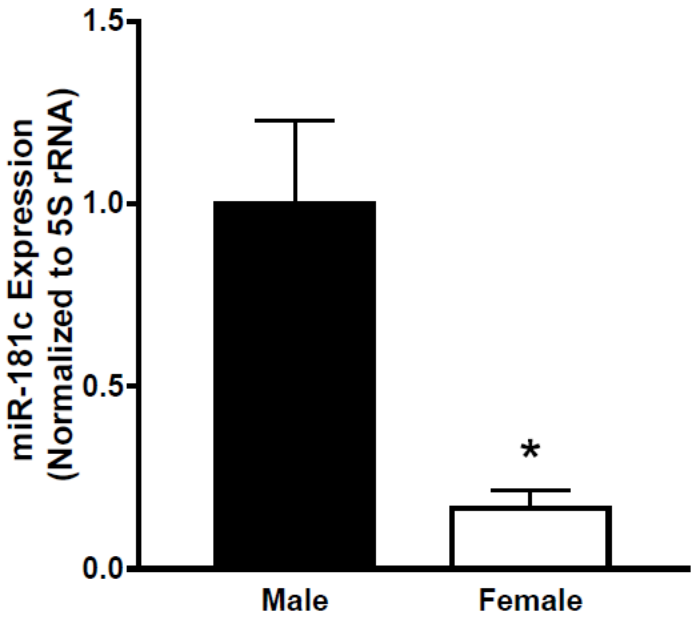

Figure S4. Sex differences in miR-181c expression in the heart. Quantitative PCR (SYBR) was performed from the RNA fractions of SD male and SD female rat hearts. miR-181c expression was normalized to 5S rRNA expression.

*p<0.05 vs. male. n=3.